Immunization of mice with chimeric antigens displaying selected epitopes confers protection against intestinal colonization and renal damage caused by Shiga toxin-producing *Escherichia coli* (STEC).

David A. Montero[1,2], Felipe Del Canto[1], Juan C. Salazar[1], Sandra Cespedes[1], Leandro Cádiz[1], Mauricio Arenas-Salinas[3], José Reyes[4], Ángel Oñate[4], Roberto M. Vidal [1,5 *]

1. Programa de Microbiología y Micología, Instituto de Ciencias Biomédicas, Facultad de Medicina, Universidad de Chile, Santiago, Chile
2. Programa Disciplinario de Inmunología, Instituto de Ciencias Biomédicas, Facultad de Medicina, Universidad de Chile, Santiago, Chile
3. Centro de Bioinformática y Simulación Molecular, Facultad de Ingeniería, Universidad de Talca, Talca, Chile
4. Departamento de Microbiología, Facultad de Ciencias Biológicas, Universidad de Concepción, Concepción, Chile
5. Instituto Milenio de Inmunología e Inmunoterapia, Facultad de Medicina, Universidad de Chile, Santiago, Chile

* Corresponding author. Correspondence should be addressed to R.V. (email: rvidal@uchile.cl)

Keywords: Shiga toxin-producing *Escherichia coli*, STEC, chimeric antigen-based vaccine, Hemolytic uremic syndrome.

Abstract

Shiga toxin-producing *Escherichia coli* (STEC) cause diarrhea and dysentery, which may progress to hemolytic uremic syndrome (HUS). Vaccination has been proposed as a preventive approach against STEC infection; however, there is no vaccine for humans and those used in animals reduce but do not eliminate the intestinal colonization of STEC. The OmpT, Cah and Hes proteins are widely distributed among clinical STEC strains and are recognized by serum IgG and IgA in patients with HUS. Here, we develop a STEC vaccine candidate based on two chimeric antigens containing epitopes of OmpT, Cah and Hes proteins. Intramuscular and intranasal immunization of mice with these chimeric antigens elicited systemic and local long-lasting humoral responses. However, the class of antibodies generated was dependent on the adjuvant and the route of administration. Moreover, while intramuscular immunization with the combination of the chimeric antigens conferred protection against colonization by STEC O157:H7, the intranasal conferred protection against renal damage caused by STEC O91:H21. This study strongly supports the potential use of this vaccine candidate as a preventive strategy against STEC infections.

Introduction

Shiga toxin-producing *Escherichia coli* (STEC) are a group of food-borne pathogens causing acute and bloody diarrhea, which may progress to life-threatening complications such as hemolytic uremic syndrome (HUS).[1] To date there is no specific treatment for STEC infection and antibiotic use is contraindicated due to increased risk of HUS development.[2] While STEC O157:H7 is the serotype most frequently associated with diarrhea outbreaks and HUS cases worldwide, there are other serotypes, the incidence and impact of which on public health and the food industry have increased.[3,4]

STEC colonizes the human colon and produces Shiga toxins (Stx) that can enter the blood stream and disseminate to organs such as the kidneys and central nervous system. Once Stx reach the target organs and enter the cells, the toxins inhibit protein synthesis, leading to autophagy and apoptosis and ultimately tissue damage, which may lead to HUS.[5]

To colonize the human colon, STEC requires several virulence factors like those encoded in the locus of enterocyte effacement (LEE) pathogenicity island (PAI). LEE-mediated adherence causes the formation of the "attaching and effacing" lesion and loss of microvilli of the intestinal epithelial cells.[6] In addition, STEC strains lacking LEE (LEE-negative STEC) harbor other PAIs like the Locus of Adhesion and Autoaggregation (LAA), which encodes virulence factors involved in intestinal colonization.[7,8] In fact, the presence of two or more PAIs in single isolates of clinically relevant STEC serotypes is common, suggesting that the cumulative acquisition of mobile genetic elements encoding virulence factors may contribute additively or synergistically to pathogenicity.[8,9]

Vaccination of the infant population, which is the highest-risk group for STEC infections, and animal reservoirs have been proposed as a preventive approach that could reduce their incidence and prevalence. However, there is no approved STEC vaccine for humans, and commercial vaccines used in cattle reduce but do not eliminate colonization and shedding of these bacteria.[10] Therefore, the development of an effective STEC vaccine is still underway. STEC proteins involved in attachment to host tissues are eligible targets for vaccine development, as they determine initial steps during infection; however, the selection of antigens that may provide a broadly and protective immune response among their diverse adhesion and colonization mechanisms is a pivotal point to consider.[11] An additional difficulty for the development of an effective STEC vaccine has been the lack of an animal model of infection that can reproduce the pathologies caused in humans.[12] Despite these limitations, several STEC vaccine candidates have been evaluated in laboratory animals (mice, rats and rabbits) and in cattle, with promising

108 results. They include Stx subunit-based vaccines,[13–15] protein and peptide-based
109 vaccines,[15–19] attenuated bacteria-based vaccines,[20] bacterial ghost-based vaccines,[21]
110 DNA-based vaccines,[22,23] and more recently nanoparticle-based vaccines.[24] While most
111 of these vaccine candidates are based on LEE-encoded antigens and Stx subunits, there
112 are several antigens encoded outside LEE that are expressed *in vivo* during human
113 infection that could be suitable targets for vaccine development.[11,25]

114 For instance, Outer membrane protease T (OmpT) and Calcium binding antigen 43
115 homologue (Cah) proteins have been shown to be recognized by IgG and IgA antibodies
116 present in sera from patients who develop HUS (hereinafter referred to as HUS sera).
117 Notably, the *ompT* gene has been identified in almost all clinical STEC strains and, in
118 the case of the *cah* gene, its detection frequency is higher than 70%.[11] Another promising
119 antigen is the Hemagglutinin from STEC (Hes), which is recognized by IgG present in
120 HUS sera.[11] In addition, the *hes* gene, which is carried by the LAA PAI, is identified in
121 about 40% and 46% of LEE-negative STEC strains isolated from humans and cattle,
122 respectively.[7,8,26] Thus, these three antigens are widespread among clinical STEC
123 strains, but it is also important to note that they are mostly absent in commensal *E. coli*
124 strains,[7,8,11] which could diminish the probability of cross-reactivity with commensal
125 microbiota. Nevertheless, the production and purification of outer membrane proteins
126 (OMPs) such as OmpT, Cah and Hes poses a challenge due to their partially
127 hydrophobic surfaces, flexibility and lack of stability that affect their solubility and efficient
128 purification. In addition, strong detergents are used in the purification of this class of
129 proteins and therefore the loss of conformational epitopes may impair their antigenicity
130 and efficiency as immunogens.[27]

131 To circumvent these issues and to develop a novel STEC vaccine targeting the OmpT,
132 Cah and Hes proteins, we implemented a vaccine development approach based on the
133 identification of linear B-cell epitopes for the design of chimeric antigens that include
134 them. Here we demonstrate that the immunization of mice with chimeric antigens
135 displaying selected epitopes of OmpT, Cah and Hes proteins induces immune responses
136 that reduce intestinal colonization and prevent renal damage caused by STEC. Overall,
137 this study revealed the feasibility of using such vaccines against STEC and other
138 pathogens. We anticipate that our comprehensive experimental approach will contribute
139 to the development and evaluation of future chimeric antigen-based vaccines.

140

141

142

143 **Results**

144 **The OmpT, Cah and Hes proteins have several linear B-cell epitopes that are**
145 **recognized by IgG and IgA from HUS sera but not from control sera.**
146
147 An overview of our vaccine development approach is shown in Figure 1. We carried out
148 a high-throughput screening of linear B-cell epitopes in the OmpT, Cah and Hes proteins
149 by using a peptide microarray assay (see Methods). A total of 6, 6 and 5 epitope-like
150 spot patterns were identified in the peptide slides of OmpT, Cah and Hes proteins (**Fig.**
151 **2a-2c**), respectively. As a complementary approach, we used a number of
152 immunoinformatics tools and found that 13 out of 17 of the experimentally identified B-
153 cell epitopes were predicted *in silico* by one or more algorithms (**Table 1**). This result
154 highlights the advances in the accuracy of these bioinformatics tools. On the other hand,
155 it is known that MHC class II (MHC-II) epitopes included in peptide vaccines enhance T-
156 cell-dependent antibody responses [28]. Thus, we also performed an *in silico* analysis for
157 the prediction of MHC-II binding peptides and found two putative T-cell epitopes in the
158 OmpT and Cah proteins (**Table 2**).
159
160 Because the peptide microarray assay was performed with a mix of three HUS sera, we
161 sought to confirm the reactivity of these epitopes using a larger number of sera. We also
162 tested the reactivity of the epitopes against three sera obtained from children with no
163 medical record of STEC-related disease (hereinafter referred to as control sera). For this,
164 short peptides ranging from 15 to 24 amino acids (aa) which include each epitope were
165 chemically synthesized, and their reactivity to IgG and IgA was assessed by ELISA. In
166 general, the peptides were recognized at higher levels by IgG than by IgA from HUS sera
167 (**Fig. 2d-i**). Furthermore, the peptides derived from the same antigen were recognized
168 by similar levels of IgG or IgA, with the exception of Cah_5 and Hes_5, which showed a
169 higher level of reactivity to IgG compared to Cah_4 and Hes_4, respectively (**Fig. 2f and**
170 **2h**). The frequency of reactivity of the peptides to IgG ranged from 60% (Hes_4) to 100%
171 (Cah_5, Cah_6 and Hes_5), while for IgA it was between 29% (Cah_2) and 100%
172 (Hes_5) (**Table 1**). As expected, a polyclonal antibody response was observed within
173 individuals, evidenced by the variable concentration of IgG and IgA antibodies that
174 recognize each tested peptide (**Fig. 2j-k**). Importantly, none of the peptides was
175 recognized by IgG or IgA from control sera (**Table 1, Fig. 2j-k**). Taken together, these
176 results indicate that the identified linear B-cell epitopes are broadly recognized and
177 immunodominant during immune responses against STEC.

178 **Chimeric proteins displaying linear B-cell epitopes of OmpT, Cah and Hes proteins**
179 **are recognized by IgG and IgA from HUS sera but not from control sera.**
180
181 We consider that the best epitopes for vaccine development are those that are
182 conserved, broadly distributed among clinical isolates, with higher levels of reactivity and
183 surface exposition in the native antigen. Consequently, the Hes_4 (lower reactivity and
184 detection frequency) and OmpT_5 (limited surface exposition) epitopes were discarded
185 and not used in further assays. For the *in silico* design of proteins we implemented two
186 different approaches. Firstly, we noticed that the linear B-cell epitopes of OmpT and Hes
187 are overlapped or consecutively arranged along the protein (**Fig. 2a and 2c**), suggesting
188 that they form antigenic domains (AD). We took advantage of this and designed a
189 chimeric protein containing these AD through the fusion of 135 AA and 127 AA from
190 OmpT and Hes proteins, respectively (**Fig. 3a**). We named this protein Chimera 1 (Chi1;
191 262 AA and 29 kDa), which includes a total of eight B-cell epitopes (OmpT_1, OmpT_2,
192 OmpT_3, OmpT_4, Hes_1, Hes_2, Hes_3 and Hes_5) and two predicted T-cell epitopes
193 (**Table 2**). In the second approach, we used the passenger domain of Cah (αCah) as a
194 carrier (keeping its epitopes) and incorporated several B-cell epitopes of OmpT and Hes
195 (**Table 2, Fig. 3d**). Thus, this second protein named Chimera 2 (Chi2; 559 AA and 56
196 kDa) includes a total of eleven B-cell epitopes (OmpT_1, OmpT_6, Hes_1, Hes_2 and
197 Hes_5, Cah_1, Cah_2, Cah_3, Cah_4, Cah_5, Cah_6) and two predicted T-cell epitopes
198 (**Table 2**).
199
200 We predicted the 3D structures for both chimeric proteins, which were refined and
201 validated (see Methods) (**Fig. 3a and 3d**). A Ramachandran plot analysis revealed that
202 94.6% and 86.6% of amino acid residues from the Chi1 and Chi2 modeled structures
203 were in favored regions, respectively (**Fig. 3b and 3e**). In addition, the Z-score of the
204 Chi1 and Chi2 modeled structures were -2.52 and -7.01 respectively, which are within
205 the range of scores found for native proteins of similar size (**Fig. 3c and 3f**). The
206 predicted solubility, *in vivo* half-life and instability index of both chimeric proteins
207 suggested that their expression and purification could be feasible (**Table 2**). Consistent
208 with the above, the production of these recombinant proteins in *E. coli* showed that they
209 are stable, water-soluble and have the predicted molecular weight (**Fig. 3g**). Further, we
210 confirm that both the Chi1 and Chi2 proteins are recognized by IgG and IgA of HUS sera
211 (**Fig. 3h and 3i**). We also found that the reactivity of Chi2 to IgG of HUS sera was
212 significantly higher than αCah (**Fig. 3h**), indicating that the incorporation of B-cell
213 epitopes of OmpT and Hes increased the seroreactivity. However, this difference was

214 not observed in the reactivity to IgA of HUS sera (**Fig. 3i**). Importantly, none of the
215 proteins was seroreactive to IgG and IgA of control sera (not shown).
216
217 **Chi1 and Chi2 antigens, administered alone or in combination, trigger long-lasting**
218 **systemic and local humoral responses in mice.**
219
220 Having established that the Chi1 and Chi2 proteins are seroreactive to HUS sera, we
221 sought to evaluate them as immunogens. For this, BALB/c mice were immunized
222 following the scheme described in Figure 1d. Immunity achieved by vaccination is
223 influenced to a large extent by the administration route and the type of adjuvant[29–31].
224 Therefore, we also compared systemic and local immune responses triggered by the
225 chimeric antigens when administered with Imject Alum or Sigma adjuvants by
226 intramuscular or intranasal route, respectively.
227
228 The measurement of Chi1 and Chi2-specific IgG antibodies in serum showed that mice
229 immunized with Chi2 or Chi1 plus Chi2 by either intramuscular or intranasal route elicited
230 significantly higher levels of IgG on days 28 and 42 than the PBS control group (**Fig. 4a**).
231 In general, intramuscular immunization induced higher levels of specific IgG antibodies
232 than the intranasal route, this difference being significant in mice immunized with Chi1
233 plus Chi2. Similarly, specific IgA antibodies in serum were significantly higher in mice
234 immunized with Chi2 or Chi1 plus Chi2 by both administration routes on days 14, 28 and
235 42 than in the PBS control group (**Fig. 4b**). It was also observed that intramuscular
236 immunization with Chi1 plus Chi2 induced higher levels of specific IgA antibodies than
237 the intranasal route, this difference being significant on day 42. In contrast, there were
238 no differences on the levels of specific IgG and IgA antibodies in serum between mice
239 immunized with Chi1 and the PBS control group (**Fig. 4a-b**). Regarding specific IgM
240 antibodies in serum, all vaccine formulations and administration routes induced
241 significant higher antibody levels on days 14, 28 and 42 than the PBS control group (**Fig.**
242 **4c**).
243
244 To evaluate the induction of mucosal responses, specific secretory IgA (sIgA) antibodies
245 were determined in feces. Mice immunized with Chi1 and Chi1 plus Chi2 by intranasal
246 route elicited significantly higher levels of specific sIgA on days 14 and 28 than the PBS
247 control group (**Fig. 4d**). However, the sIgA levels for both experimental groups were
248 similar on day 42 compared to the PBS control group. On day 42, only mice immunized
249 with Chi2 by intranasal route elicited significantly higher levels of specific sIgA than the
250 PBS control group. Taken together, these results indicate that immunization with Chi1,

251 Chi2 or Chi1 plus Chi2 induces long-lasting systemic and local humoral responses
252 influenced by the type of adjuvant and the administration route.
253
254 **Chi1 and Chi2 antigens administered in combination by intramuscular route**
255 **reduce intestinal colonization and fecal shedding of STEC O157:H7**
256
257 We next evaluated whether immune responses elicited by vaccination with the chimeric
258 antigens may confer protection against intestinal colonization by STEC. For this, two
259 weeks after the last booster immunization, mice were treated with streptomycin and then
260 orally challenged with STEC O157:H7 str. 86-24 (**Fig. 1d;** see Methods). Notably, mice
261 immunized with Chi1 plus Chi2 by intramuscular route showed a significantly lower fecal
262 shedding of the STEC 86-24 strain from day 8 post-infection to the end of the experiment
263 (day 12) compared to the PBS control group (**Fig. 5a**). In mice immunized by the
264 intranasal route, only the Chi2 group showed a slight but significant decrease in fecal
265 shedding of STEC 86-24 strain on days 7 and 8 compared to the PBS control group.
266 However, on day 9 and later, this difference was not observed (**Fig. 5b**).

267 On day 12 post-infection, mice were euthanized and the level of colonization of the
268 challenge strain in the cecum was determined. Consistent with the above results,
269 recovery of the STEC 86-24 strain was significantly lower in mice immunized with Chi1
270 plus Chi2 by intramuscular route than in the PBS control group, which corresponded to
271 2.1 log of protection (**Table 3**). The other experimental groups presented levels of
272 colonization similar to the PBS control group. These data demonstrate that immunization
273 of mice with Chi1 plus Chi2 by intramuscular route induces protective immune responses
274 against intestinal colonization of STEC O157:H7.

275
276 **Chi1 and Chi2 antigens administered alone or in combination by intranasal route**
277 **avoid renal damage caused by STEC O91:H21**
278
279 Kidney damage is one of the most severe clinical outcomes that can occur during STEC
280 infection due to the action of Shiga toxins. In streptomycin-treated mice, Stx2d-producing
281 *E. coli* strains have been shown to affect renal function leading to death.[32,33] For instance,
282 in a previous study we showed that the Stx2d-producing *E. coli* O91:H21 str. V07-4-4 is
283 lethal to mice when they are orally inoculated with a dose of 10^9 CFU.[8] However, with a
284 dose lower than 10^5 CFU of the STEC V07-4-4 strain, mice develop renal pathologies
285 but survive for at least 12 days (unpublished results). Therefore, we conducted further
286 work to investigate whether immunization with the chimeric antigens confers protection

287 against renal damage caused by the STEC V07-4-4 strain. For this, two weeks after the
288 last booster immunization, mice were treated with streptomycin and orally challenged
289 with 10^5 CFU of the STEC V07-4-4 strain. Our results showed that on days 7 and 12
290 post-infection, mice intranasally immunized with Chi1, Chi2 or Chi1 plus Chi2 had
291 creatinine levels in urine similar to uninfected mice (**Fig. 5c and 5d**). This was particularly
292 evident in mice immunized with Chi1 plus Chi2. In contrast, mice immunized by
293 intramuscular route and the PBS control group showed significantly higher levels of
294 creatinine in urine than uninfected mice. Moreover, the histopathological analysis of
295 kidney tissue obtained on day 12 post-infection showed that mice immunized by
296 intranasal route had mild or no evident tissue injuries (**Fig 5e**). Conversely, mice
297 immunized by intramuscular route and the PBS control group showed moderate and
298 severe tissue injuries, respectively (**Fig 5e**). Urinary clinical markers such as the number
299 of leukocytes and urobilinogen levels on day 12 post-infection also evidenced the
300 protection achieved by intranasal immunizations (**Table 4**). Together, these results
301 indicate that immunization with the chimeric antigens by intranasal route protects against
302 kidney damage caused by the STEC V07-4-4 strain.
303
304
305
306
307
308
309
310
311
312
313
314
315
316
317

318 **Discussion**

319 Here we demonstrated that immunization of mice with chimeric antigens displaying
320 selected epitopes of OMPs confers protection against intestinal colonization and renal
321 damage caused by STEC. It is well established that a suitable vaccine must be
322 composed of different antigens to boost the immune response with a wide range of
323 protection. Thus, since the OmpT, Cah and Hes proteins are widespread among STEC
324 strains, the use of these proteins as targets could confer protection against LEE-positive
325 and LEE-negative STEC strains. To our knowledge, this is the first STEC vaccine
326 candidate that includes a virulence factor of LEE-negative STEC strains.

327 In general, subunit and protein-based vaccines have proven to be safe and to have a
328 defined and homogeneous composition between production batches. This is an
329 important advantage over other types of vaccines, which may present complex
330 manufacturing processes, with subsequent regulatory and safety issues.[34–36] In Gram-
331 negative bacteria, OMPs are primary components interacting with host cells; therefore,
332 vaccines targeting these proteins may be effective by blocking key pathogenic
333 mechanisms.[11,37] However, as previously mentioned, the purification and efficient
334 production of OMPs pose a major challenge. Thus, construction of water-soluble and
335 stable chimeric antigens displaying epitopes from OMPs is an approach worth exploring.

336 Our vaccine development approach takes advantage of immunoinformatics tools and *in*
337 *vitro* assays (epitope mapping, ELISA) to predict and identify linear B-cell epitopes,
338 respectively (**Fig. 1**). Previous studies have also demonstrated the usefulness of
339 immunoinformatics tools for the development of vaccine candidates against STEC and
340 other pathogens.[22,38] Additional work conducted to evaluate the seroreactivity of the
341 epitopes using a large set of HUS sera allowed us to select the best epitopes based on
342 their frequency and level of reactivity (**Fig. 2, Table 1**). Another important parameter we
343 considered for the selection of epitopes was the surface exposition in the native antigen,
344 which could facilitate their recognition by immune cells. Predicted T-cell epitopes were
345 also included in the structure of chimeric proteins to enhance T-cell-dependent antibody
346 responses (**Table 2**).

347 Importantly, our results provide proof-in-principle that incorporating selected linear B-cell
348 epitopes into a carrier protein, such as aCah, may result in an increase in antigenicity
349 (**Fig. 3h**). Many autotransporter (AT) proteins and especially their passenger domains
350 are potential vaccine targets.[39,40] In fact, the pertactin AT from *Bordetella pertussis* is a
351 component of licensed pertussis vaccines.[41] Thus, other passenger domains from AT
352 proteins could be used as carriers to design chimeric antigens.

353 The immunization studies showed that the Chi1 and Chi2 antigens, administered alone
354 or in combination, induce long-lasting humoral responses (**Fig 4**). However, the class of
355 antibodies generated was in general dependent on the adjuvant and the administration
356 route. This dependency was most obvious in mice immunized with Chi1 plus Chi2, which
357 elicited significantly higher levels of specific IgG and IgA antibodies in serum when
358 intramuscularly immunized than when intranasally immunized (**Fig. 4a-b**). Conversely,
359 the intranasal but not the intramuscular administration of Chi1 plus Chi2 led to the
360 production of significant levels of fecal sIgA compared to the PBS control group (**Fig.**
361 **4d**).

362 Secretory IgA is the most abundant immunoglobulin of the mammalian mucosa, playing
363 a fundamental role in the immunity of the gastrointestinal tract.[42] Therefore, the
364 development of vaccines against intestinal pathogens has traditionally given priority to
365 immunogens that induce significant levels of sIgA. However, since some gastrointestinal
366 infections can be eliminated in the absence of sIgA; other classes of antibodies such as
367 IgM and IgG may also play an important role in the intestinal immunity.[43] Unfortunately,
368 the presence and effector functions of IgG in the intestinal mucosa have been largely
369 ignored in the literature.[44] A recent study by Kamada et al., 2015,[45] revealed that IgG in
370 the murine intestine leads to the selective elimination of a virulent *Citrobacter rodentium*
371 subpopulation by luminal neutrophils. The protective role of IgG against other
372 enteropathogens such as rotavirus has also been demonstrated.[46] Our challenge
373 experiments using the STEC O157:H7 strain showed that only immunization with Chi1
374 plus Chi2 by intramuscular route confers protection against intestinal colonization (**Fig.**
375 **5a-b, Table 3**). Since intramuscular immunization with Chi1 plus Chi2 did not lead to
376 significant production of specific fecal sIgA antibodies (**Fig. 4d**), it is possible to correlate
377 the protection achieved with other classes of immunoglobulins and more likely with the
378 IgG. Other vaccine candidates that generated significant levels of specific IgG antibodies
379 in serum but not fecal sIgA antibodies have also conferred protection to mice against
380 colonization by STEC O157:H7.[47] Consequently, our results and those reported by
381 others support the idea of a pivotal role of the IgG antibodies in the defense against
382 enteropathogens. This is a major finding that will be relevant to the development of
383 vaccines against these pathogens by avoiding biases in the selection of the "best"
384 immunogens based mainly on the ability to induce sIgA antibody responses.

385 Because the challenge studies were performed only to day 12 post-inoculation, it was
386 not possible to determine whether the immune responses triggered by the intramuscular
387 immunization with Chi1 and Chi2 may lead to complete clearance of STEC O157:H7.

388 Long-term protection experiments in mice and other animal models will complement the
389 evaluation of this vaccine candidate.

390 An effective STEC vaccine may also confer protection against the action of the Stx.
391 STEC export the Shiga toxins along with a number of OMPs and cytoplasmic proteins
392 via outer membrane vesicles (OMVs).[48–50] These OMVs may be endocytosed in a
393 dynamin-dependent manner by intestinal epithelial cells, and then OMV-associated
394 virulence factors are differentially separated from vesicles during intracellular trafficking.
395 [50,51] Recently, it was reported that in the case of Stx2 but not Stx1, once the toxin is
396 internalized, it can be released from eukaryote cells in microvesicles that have exosome
397 markers.[52] Therefore, immunity against Stx may be mediated by neutralizing Stx-specific
398 antibodies or by immune mechanisms that prevent the toxin from entering the eukaryotic
399 cell.

400 Our chimeric antigens did not display Stx-associated epitopes. Consequently, the
401 protection conferred by intranasal immunizations against renal damage caused by STEC
402 O91:H21 (**Fig. 5c-e, Table 4**) could be explained by two different mechanisms. The first
403 one, which is the simplest explanation, is that the generated immune response
404 decreased the intestinal colonization of the STEC O91:H21 strain, which could be
405 correlated with a lower release and amount of OMVs and Stx. However, in the challenge
406 experiments with the STEC O157:H7 strain, only intramuscular immunization with Chi1
407 plus Chi2 was able to confer protection against intestinal colonization (**Fig. 5a and 5b**).
408 In addition, because the levels of intestinal colonization of the STEC O91:H21 strain
409 were not measured, we cannot conclude that in our experiments a decrease in
410 colonization correlates with protection against renal damage. The second possible
411 explanation, although a bit more complex, is that sIgA antibodies generated by intranasal
412 immunizations could prevent the release and/or the endocytosis of OMVs via immune
413 exclusion. The latter explanation is supported by the fact that OmpT and Ag43 (a Cah
414 homologue protein) are transported in OMVs.[51,53] In fact, it has been reported that OmpT
415 regulates the biogenesis of OMVs.[54]

416 In some vaccines, it has been shown that the combination of administration routes, for
417 example mucosal priming followed by systemic boosting or systemic priming followed by
418 mucosal boosting, leads to robust humoral and cellular responses that improve their
419 efficacy.[55,56] In future studies we will investigate whether the combination of systematic
420 and mucosal immunizations with the Chi1 and Chi2 antigens leads to a more robust and
421 complete immune response characterized by the production of both systemic and
422 secretory antibodies. Also, we will endeavor to reveal the mechanism by which intranasal

immunization with Chi1 and Chi2 confers protection against renal damage caused by STEC O91:H21.

In conclusion, we developed a promising STEC vaccine candidate that confers protection against intestinal colonization and renal damage. Our results strongly support the potential use of this vaccine as a preventive strategy against STEC infections.

450 **Materials and methods**

451 **Bacterial strains and growth conditions**

452 Spontaneously derived streptomycin resistant (Str^r) mutants of STEC O157:H7 86-24
453 and STEC O91:H21 V07-4-4 strains were used in this study. Bacterial cultures were
454 routinely grown at 37 °C in Luria-Bertani (LB) broth.

455

456 **Human sera**

457 Sera were obtained from 20 pediatric patients in the convalescent phase who presented
458 diarrhea within two weeks prior to HUS diagnosis (HUS sera). Control sera were
459 obtained from two patients with no history of STEC-associated diarrhea. These sera
460 were collected from 1990 to 1993 and from 1999 to 2003 in various healthcare centers
461 in Santiago, Chile, with the informed consent of the parents or legal guardians. All
462 procedures were approved by the Ethics Committee of the Facultad de Medicina,
463 Universidad de Chile.

464

465 **Peptide Microarray**

466 Epitope mapping assays were performed by PEPperPRINT (Heidelberg, Germany).
467 Briefly, the *ompT*, *cah* and *hes* sequences were translated into 15, 12 and 10 amino acid
468 peptides with peptide-peptide overlaps of 14, 11 and 9 amino acids. The microarray
469 contained peptides printed in duplicate framed by HA (YPYDVPDYAG) control peptides.
470 Peptide slides were incubated with a mix of three HUS sera at a dilution of 1:100 followed
471 by secondary antibody Goat anti-human IgA (DyLight800) at a dilution of 1:1000, in the
472 presence of the monoclonal anti-HA (12CA5)-DyLight680 control antibody at a dilution
473 of 1:2000. The read-out was performed with a LI-COR Odyssey Imaging System and the
474 image analysis with the PepSlide® Analyzer.

475

476 ***In silico* prediction of B-cell and T-cell epitopes**

477 Prediction of B-cell epitopes was done using several tools available at the IEDB server
478 [57], including BepiPred 2.0 [58], Kolaskar and Tongaonker antigenicity method [59] and Ellipro
479 [60]. Peptides binding to MHC-II molecules were also predicted on the IEDB server [57].

480

481 **Validation of epitopes by ELISA assay**

482 Seventeen short peptides from 15 to 24 amino acids (**Table 1**) containing linear B-cell
483 epitopes were chemically synthesized at Genic Bio Ltd (Shanghai, China). These short
484 peptides were evaluated for their reactivity to IgG and IgA of individual HUS sera by
485 ELISA. Briefly, 96-well ELISA plates (Nunc Maxisorp or Nunc Immobilizer Amino Plates,

486 ThermoFisher, USA) were incubated with 1.2 µg of each peptide diluted in 100 µl of
487 phosphate-buffered saline (PBS; pH 7.2) overnight at 4 °C. Standard curves were
488 obtained by dilutions in PBS of purified human IgG (Cat. 02-7102, Invitrogen, USA) or
489 IgA (Cat. 3860-1AD-6, Mabtech, USA) ranging from 1.2 µg/ml to 0,0047 µg/ml. Plates
490 were washed three times with PBS containing 0.05% Tween 20 (TPBS) and then
491 incubated with blocking solution (TPBS + 0.5% bovine serum albumin) for 15 min at room
492 temperature (RT). The HUS and control sera were diluted 1:25 (dilution determined from
493 serum titration experiments in a range of 1:10 to 1:100) in blocking solution (100 µl / well)
494 and incubated for 60 min at 37 °C. After six washes with T-PBS, goat anti-human IgG (H
495 + L), peroxidase-labeled (Cat. 04-10-06, KPL, USA) or goat anti-human IgA alpha chain
496 (alkaline phosphatase) (Cat. Ab97212, Abcam, UK), diluted 1:1000 in blocking solution,
497 were added and plates were incubated for 60 min at 37 °C. After six washes with Tris-
498 buffered saline (TBS; pH 7.5) containing 0.05% Tween 20, ABTS® peroxidase substrate
499 (Cat. 50-66-18, KPL, USA) or pNPP substrate (Cat. N2600-10, USBiological, USA) were
500 added and plates were incubated for 12 or 30 min at RT, respectively. The reaction was
501 stopped with 5% sodium dodecyl sulfate or 3M sodium hydroxide dissolved in distilled
502 water. The absorbance was determined at 405 nm (A_{450}) using a Synergy HT microplate
503 reader (Biotek Instruments, USA). Each sample was determined twice in duplicate. The
504 relation between absorbance values and the IgG or IgA concentration of each well was
505 calculated from standard curves using a four-parameter logistic regression in GraphPad
506 Prism 8 software.
507
508 ***In silico* modeling and design of chimeric proteins**
509 Predicted three-dimensional structure of Chimera 1 was constructed based on the crystal
510 structures of the Opa60 (PDB_ID: 2MLH)[61] and OmpT (PDB_ID: 1I78)[62] proteins. The
511 template for Chimera 2 structure was the crystal structure of the Ag43 protein (PDB_ID:
512 4KH3).[63] Comparative modeling of chimeric proteins was performed in Modeller v9
513 software[64], using default parameters. The modeled structures were solvated and
514 embedded in a water box using ions (Na+, Cl-) to neutralize the system with the TCL
515 script using VMD software.[65] The models were optimized with cycles of energy
516 minimization and dynamics using the NAMD 2.12 software.[66] A molecular dynamics
517 simulation was performed under periodic bordering conditions and isobaric-isothermal
518 set (NPT). The entire system was relaxed by molecular dynamics (MD) simulations using
519 NAMD 2.12 software for 10 ns and subsequently balanced for 30 ns, using the force field
520 CHARMM v2.7.[67] Quality evaluation and validation of the models were carried out by
521 Ramachandran plot analysis on the RAMPAGE server
522 (http://mordred.bioc.cam.ac.uk/~rapper/rampage.php) and ProSA-web.[68] Chemical and

523 physical properties of the chimeric proteins were predicted by Protein-Sol[69] and
524 ProtParam[70] tools. The modelled structures were visualized with UCSF Chimera
525 1.10.2.[71]
526
527 **Purification of proteins**
528 Synthetic genes and production of Chimera 1, Chimera 2 and αCah proteins were
529 ordered to GenScript (USA). Synthetic genes were optimized for *E. coli* expression and
530 cloned into vector pET30a with N-terminal 6xHis-tag. *E. coli* strain BL21(DE3) was then
531 transformed with recombinant plasmids containing synthetic genes. For purification of
532 recombinant proteins, transformant BL21(DE3) strains were grown in Terrific Broth
533 containing kanamycin (50 µg/ml) at 37° C. When the culture reached an optical density
534 at 600 nm of ~1.2, it was supplemented with IPTG for 4 h. Later, cells were harvested by
535 centrifugation, resuspended with lysis buffer followed by sonication. The sediment
536 obtained after centrifugation was dissolved using urea. Denatured protein was obtained
537 by one-step purification using a Ni-column. The target protein was refolded and sterilized
538 by 0.22 µm filter before being stored in aliquots. The concentration was determined by
539 Bradford protein assay with BSA as standard. The protein purity and molecular weight
540 were determined by standard SDS-PAGE along with Western blot confirmation. Target
541 proteins were obtained with purity >85% and endotoxin level <2 EU/mg (LAL Endotoxin
542 Assay Kit, GenScript, Cat. No. L00350). In addition, reactivity of Chimeric and αCah
543 proteins to IgG and IgA of individual HUS was assessed by ELISA assay as described
544 above.
545
546 **Immunization studies**
547 All animal experiments were performed at the Universidad de Concepción, Concepción,
548 Chile, following protocols and guidelines approved by the Bioethics Committee of the
549 Faculty of Biological Sciences. Female BALB/c mice (5 to 6 weeks old; purchased from
550 the Instituto de Salud Pública, Santiago, Chile) were randomly distributed into seven
551 experimental groups (each group n=20) and housed in conventional animal facilities with
552 water and food *ad libitum*. Mice were anesthetized with 10 mg/ml of ketamine and 250
553 µg/ml of acepromazine and immunized by intramuscular (i.m.) or intranasal (i.n.) route
554 with the corresponding protein formulation along with 50 µl of Imject™ Alum Adjuvant
555 (ThermoFisher Scientific, USA) or 20 µl of Sigma Adjuvant System® oil (Sigma-Aldrich,
556 USA), respectively (**Fig. 1d**). Experimental groups 1, 3 and 5 were i.m. immunized with
557 either 20 µg of Chi1, 20 µg of Chi2 or 10 µg of Chi1 plus 10 µg of Chi2, respectively.
558 Experimental groups 2, 4 and 6 were i.n. immunized with either 20 µg of Chi1, 20 µg of
559 Chi2 or 10 µg of Chi1 plus 10 µg of Chi2, respectively. The control group were injected

560 with PBS plus adjuvants. Two booster immunizations were performed on days 15 and
561 30 using similar amounts of protein formulations and adjuvants.
562
563 **Sera and feces collection**
564 Sera were obtained from five mice per group by tail vein bleeding on days -2, 14 and 28
565 before each immunization and at day 42 (two weeks after the last booster immunization),
566 according to conventional techniques. Briefly, blood samples were left at 37 °C for 30
567 min and then centrifuged at 1,000 x g for 10 min. Supernatant was collected, the
568 complement was inactivated at 56 °C for 30 min and aliquots were stored at -80 °C until
569 IgG, IgA and IgM determinations by ELISA. For secretory IgA (sIgA) measurement, feces
570 were collected on days -2, 14, 28 and 42. Feces were weight, homogenized and diluted
571 to 0.1 g/ml with PBS containing 0.1% sodium azide and 1 mM of phenylmethylsulfonyl
572 fluoride (PMSF). Fecal suspension was centrifuged at 15,000 x g for 5 min at 4 °C, the
573 supernatant fluid recovered and again centrifuged at 15,000 x g for 15 min at 4 °C and
574 stored at -80 °C until use.
575
576 **Measurement of humoral response**
577 Chimeric proteins were diluted to 1 µg/ml in carbonate buffer (pH 9.6) and used to coat
578 polystyrene 96-well high-binding ELISA plates (100 µl/well; Nunc-Immuno plate with
579 MaxiSorp surface). After overnight incubation at 4 °C, plates were washed with washing
580 buffer (Tris-buffered saline [pH 7.4] with 0.05% Tween 20) and blocked with 0.8% gelatin
581 in TPBS for 1 h at 37 °C and then incubated with either sera or supernatant from fecal
582 suspensions, at a dilution of 1:100, for 2.5 h at room temperature and washed four times.
583 Next, isotype-specific goat anti-mouse HRP conjugates (BioLegend, USA) were added
584 (100 µl/well) at a dilution of 1:1000 and incubated for 1 h min at room temperature
585 followed by washing with TPBS. Then, 200 µl/well of OPD Peroxidase Substrate (Cat.
586 P9187-5SET, Sigma-Aldric, USA) was added for 30 min. The reaction was stopped with
587 50 µl/well of 2N H_2SO_4 and the absorbance at 450 nm was measured on a microplate
588 reader.
589
590 **Challenge studies**
591 Two weeks after the last booster immunization (day 45), the infection experiments were
592 performed in the streptomycin-treated mouse model of STEC infection as described
593 elsewhere[72,73] with minor modifications. Briefly, mice were given water *ad libitum*
594 containing streptomycin (5 g/l) 24–48 h prior to inoculation and for the duration of the
595 experiment. Feces were documented to be free of streptomycin-resistant *E. coli* at the
596 time of inoculation. STEC O157:H7 86-24 and STEC O91:H21 V07-4-4 strains were

597 grown overnight in agitated LB broth containing 50 µg/ml streptomycin at 37 °C. Cultures
598 were centrifuged, washed once with PBS and resuspended in a 20% sucrose (w/v) and
599 10% NaHCO3 (w/v) solution in sterile water to 1 x 10^{10} CFU/ml (STEC 86-24 strain) or 1
600 x 10^{6} CFU/ml (STEC V07-4-4 strain). Prior to inoculation, mice were starved of food and
601 water overnight (12 h). The next morning mice were orally infected by pipette feeding
602 with 100 µl of bacterial suspension containing 10^{9} CFU or 10^{5} CFU of STEC 86-24 or
603 STEC V07-4-4 strains, respectively. After challenge, food and water were reintroduced
604 and provided *ad libitum*. The fecal shedding of the 86-24 strain was recorded daily for 12
605 days. For this, feces were collected, weighed, homogenized, suspended in 1 ml PBS
606 and, after serial dilutions, plated on MacConkey agar plates supplemented with
607 streptomycin (50 µg/ml) for bacterial counts. For determination of intestinal colonization
608 of the STEC 86-24 strain, 12 days after challenge (day 57), mice were euthanized, and
609 cecum was collected under aseptic conditions, homogenized and diluted in PBS.
610 Suspensions were serially diluted and plated on MacConkey supplemented with
611 streptomycin (50 µg/ml) for bacterial counts. Log_{10} units of protection were obtained by
612 subtracting the mean Log_{10} CFU for each experimental group from the mean Log_{10} CFU
613 of the PBS control group. Mice inoculated with the STEC V07-4-4 strain were used to
614 measure kidney damage (*vide infra*).
615
616 **Urinalysis**
617 Urine samples were collected as previously described [74], on days 45, 51 and 57 (0, 7
618 and 12 post-infection, respectively) from mice infected with the STEC V07-4-4 strain.
619 Biochemical estimation of urine creatinine concentration was assessed using the
620 Creatinine Kit (BioSystems, Spain) according to the manufacturer's instructions. Other
621 clinical urine markers were measured by using Combur10 Test®M semiquantitative test
622 strips (Roche Diagnostics GmbH, Germany). Each test strip consists of colorimetric
623 reaction spots for 10 markers: specific gravity (1.000 to 1.030), pH (5.0 to 9.0),
624 leukocytes (range, negative to 500 cells/µL), nitrites (negative or positive), proteins
625 (negative to 500 mg/dl), glucose (negative to 55 mmol/l), ketones (negative to 15
626 mmol/L), urobilinogen (normal to 200 µmol/L), bilirubin (negative to +3) and blood
627 (negative; trace of non-hemolyzed; or hemolyzed, 10 to 250 cells/µL). Each square was
628 wet with a drop of urine and the marker value was determined through comparison with
629 a colorimetric standard.
630
631 **Histopathological analysis of kidney tissue**
632 For the histological analysis of kidney tissue, mice infected with the STEC V07-4-4 strain
633 were euthanized at day 57, the kidneys collected, fixed in 10% formaldehyde (pH 6.9),

embedded in paraffin wax for sectioning at 5 μm and stained with hematoxylin and eosin (H/E). Pathological evaluation of H/E-stained tissue sections was carried out by a pathologist blinded to the experimental design. Histopathological changes were evaluated by the degree of perivascular edema, leukocyte infiltration, vascular congestion, mesangial cell expansion and injury of the glomerular filtration barrier (glomerular hypertrophy or glomerular hypoperfusion). Each sample was quantitated by ten randomly selected fields with the following criteria: 0, no damage; 1, <25%; 2, 25–50%; 3, >50%; 4, >75% of damage. Differences between experimental groups were evaluated by a one-way ANOVA followed by Tukey's multiple comparisons test.

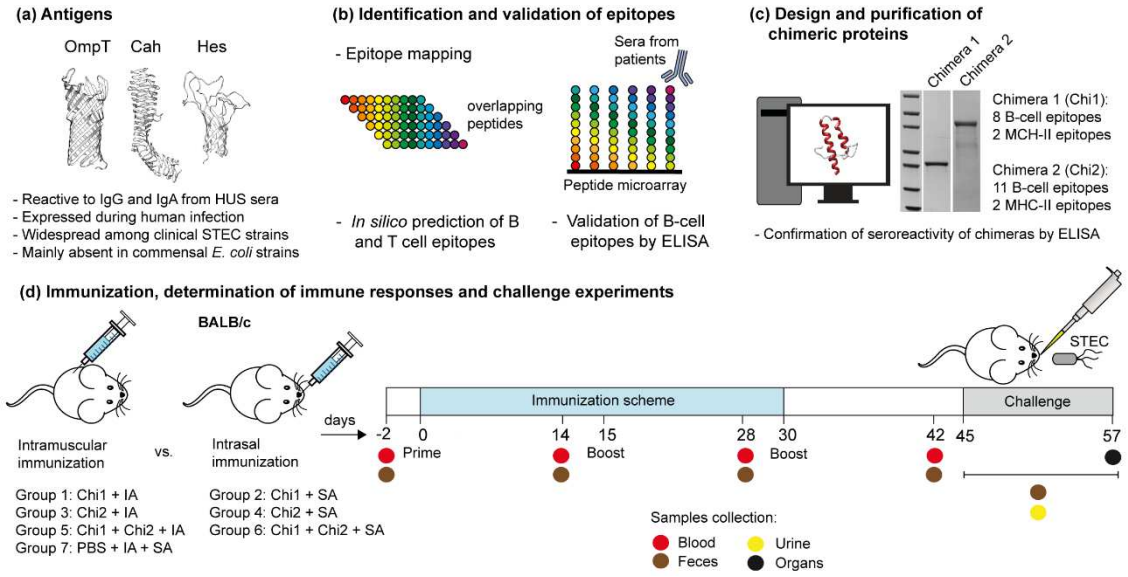

Fig. 1. Experimental design for the development and evaluation of the chimeric-based STEC vaccine. **a**) We selected the OmpT, Cah and Hes proteins as suitable targets against STEC based on their antigenic properties, frequency of detection among clinical STEC strains and absence among commensal *E. coli* strains. **b**) The proteins were analyzed by immunoinformatics tools and a peptide microarray assay for B-cell epitope prediction and mapping, respectively. MHC-II epitopes were also predicted *in silico*. Several B-cell epitopes were validated by ELISA using a collection of HUS sera. **c**) Selected epitopes were used to design two chimeric proteins that were expressed and purified. The reactivity of the chimeric proteins to IgG and IgA present in HUS sera was also confirmed. **d**) BALB/c mice were immunized with different vaccine formulations by intramuscular or intranasal route using Imject Alum (IA) or Sigma adjuvant (SA), respectively. Systemic and local humoral responses were subsequently determined. The protection conferred by immunizations was evaluated in the streptomycin-treated mouse model by challenge with STEC O157:H7 and O91:H21 strains. Bacterial shedding and intestinal colonization were determined for the STEC O157:H7 infected mice. Renal damage was examined in the STEC O91:H21 infected mice.

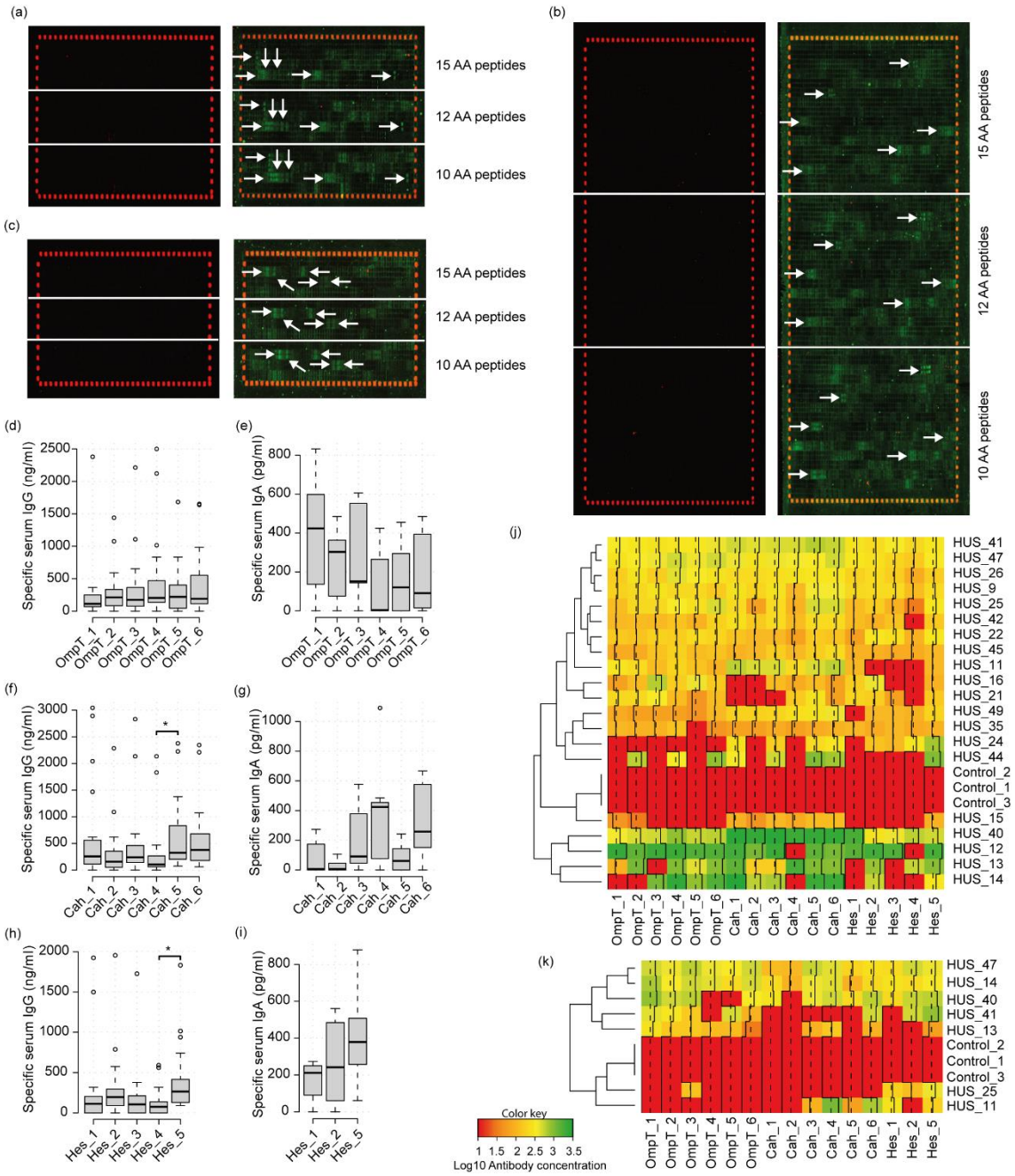

Fig. 2. Identification and validation of linear B-cell epitopes of the OmpT, Cah and Hes proteins. a, b and c) Peptide microarray assays. Peptide slides containing 15, 12 and 10 AA peptides derived from de OmpT (a), Cah (b) and Hes (c) proteins were incubated with a mix of three HUS sera at a dilution of 1:100. After washing, staining was performed with secondary anti-human IgA DyLight800 antibody at a dilution of 1:1000. Control peptides (red spots) framing the peptide slides were staining with specific monoclonal DyLight680 antibody at a dilution of 1:2000. Control peptide slides incubated with anti-human IgA DyLight800 antibody and the specific monoclonal DyLight680 antibody are shown in the left panels. Epitope-like spot patterns are indicated by white arrows. **d-i**) Tukey box plots showing concentrations of IgG and IgA present in individual HUS sera (n=20) that are reactive to short peptides containing B-cell epitopes of the OmpT, Cah and Hes proteins. A lower number of HUS sera and Hes epitopes were assessed due to sera availability. Tukey box plots show the 25th to 75th percentiles, with the median indicated by the horizontal line inside the box. Data analysis was by Kruskal-

Wallis test, followed by Dunn's multiple comparison test. *P < 0.0 5 was considered significant. **j** and **k**) Heatmaps show the logarithm of the IgG and IgA concentration of each serum (HUS or control sera) that recognizes a specific short peptide, respectively. Data were clustered hierarchically using Euclidean distance and complete linkage analyses. Each row represents a different serum and each column a specific epitope. The average (dotted line) and histogram (solid line) of the values obtained by each peptide are indicated in the columns. The color key indicates the value of the logarithm of the antibody concentration. The figure was made using the "gplots" [75] package in R [76].

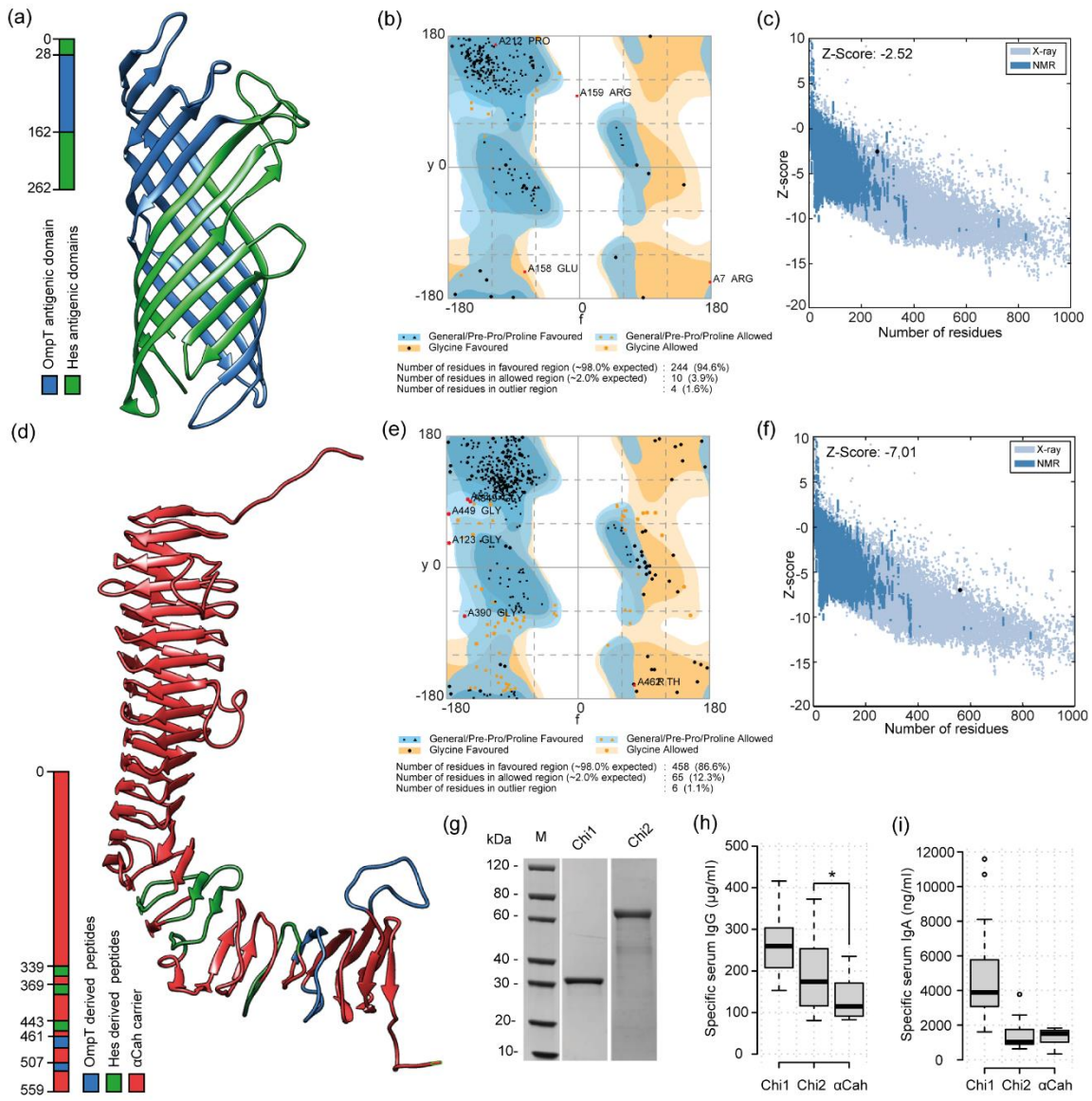

Figure 3. Design and production of the chimeric antigens. a) Predicted 3D structure of the Chimera 1 (Chi1) antigen. OmpT- and Hes-derived peptides are shown as indicated in the legend at the left. **b and c**) Quality validation of modeled Chi1 structure. Ramachandran plot (b) shows that 94.6% residues were in favored regions. Z-score plot (c) for Chi1 model obtained by ProSA-web.[68] Dark blue and light blue regions represent z-scores of native protein structures determined by NMR and X-ray, respectively. Black spot shows z-score for the Chi1 model. **d**) Predicted 3D structure of the Chimera 2 (Chi2) antigen. OmpT- and Hes-derived peptides are shown as indicated in the legend at the left. **e and f**) Quality validation of modeled Chi2 structure. Ramachandran plot (e) shows that 86.6% residues were in favored regions. Z-score plot (f) for Chi2 model. **g**) SDS-PAGE of purified Chi11 and Chi2 proteins. M, Molecular weight standard. **h-i**) Tukey box plots showing concentrations of IgG (h) and IgA (i) present in individual HUS sera (n=20) that are reactive to Chi1, Chi2 and aCah proteins. Tukey box plots show the 25th to 75th percentiles, with the median indicated by the horizontal line inside the box. Data analysis was by Kruskal-Wallis test, followed by Dunn's multiple comparison test. *P < 0.0 5 was considered significant.

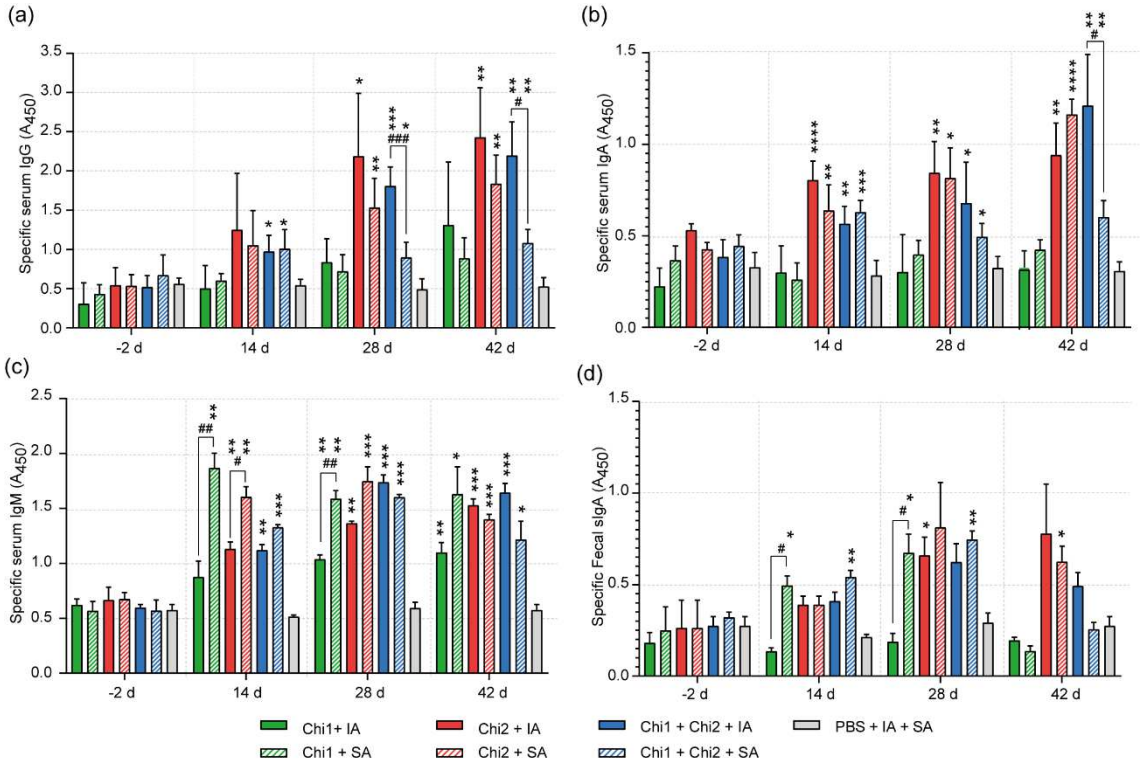

Figure 4. Humoral immune responses triggered by immunization with the chimeric antigens. Sera obtained at days -2, 14, 28 and 42 post-immunization were diluted 1:100 and used for the determination of specific IgG (a), IgA (b) and IgM (c) by ELISA. Fecal sIgA (d) was also determined from feces collected on days -2, 14, 28 and 42. The results are expressed as means ± SD of absorbance values at 450 nm (A_{450}), which were obtained from individual sera or fecal suspensions of five mice per group. Experimental groups are shown as indicated by legend at the bottom. Data analysis was by a two-way ANOVA, followed by Tukey's multiple comparison test. $P < 0.0\ 5$ was considered significant. Asterisks (*) indicate significant differences between the immunized mice and the PBS control group. Number signs (#) indicate significant differences between administration routes.

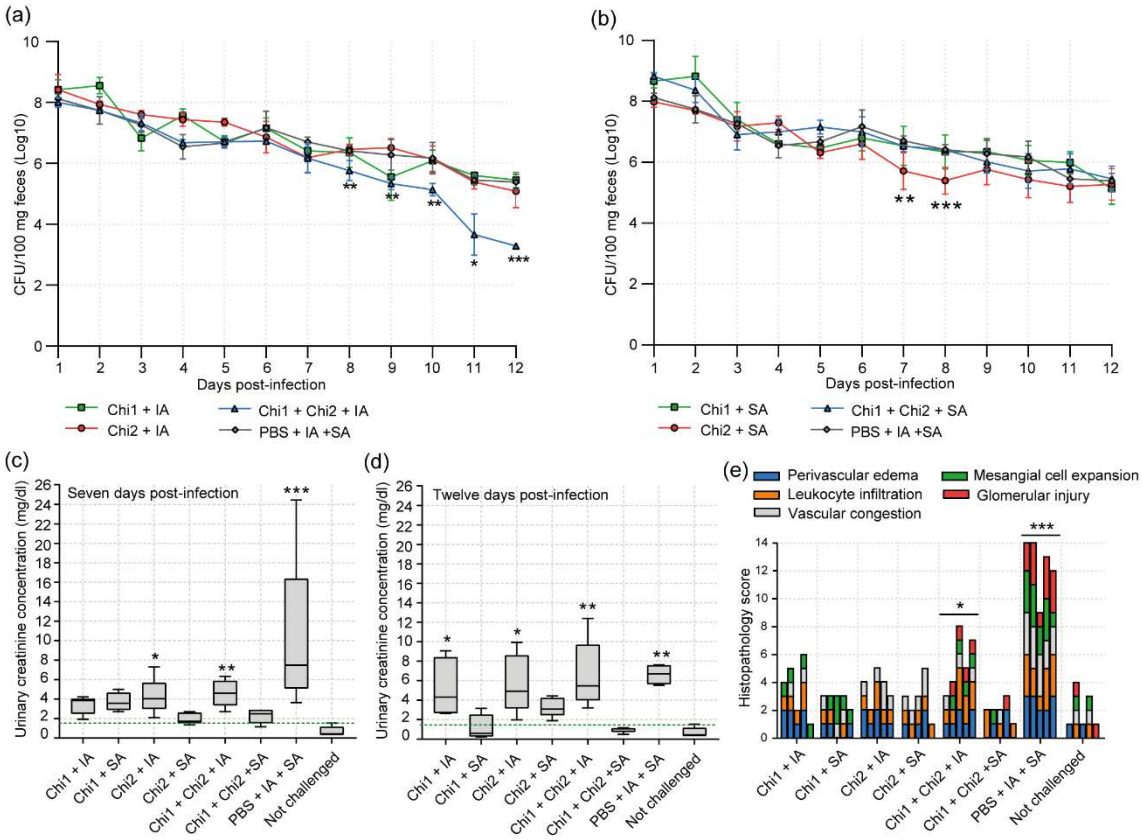

Figure 5. Protection conferred by immunizations with the chimeric antigens. a and b) Determination of fecal shedding of STEC O157:H7. Eight mice per group were orally inoculated with 10^9 CFU of the challenge strain. Fecal pellets were collected daily, weighed, homogenized, and plated on MacConkey agar containing streptomycin. Data are showed as the number of CFU of the challenge strain per 100 mg feces. Differences between immunized mice and the PBS control group were analyzed by a two-way ANOVA with Tukey's multiple comparison test. Experimental groups are shown as indicated by legend at the bottom. **c and d**) Tukey box plots showing creatinine concentrations (mg/dl) in urine determined from five mice per group on days 7 (c) and 12 (d) post-infection with STEC O91:H21. Differences between experimental groups and uninfected mice were analyzed by Mann-Whitney U test. Dotted green line indicates normal creatinine concentration of 1.5 mg/dl. **e**) Histopathology analysis from kidney tissue obtained from five mice per group on day 12 post-infection with STEC O91:H21. Cellular injuries were classified as not evident, mild, moderate or severe as described in the Methods. Cellular injuries are color coded as indicated in the legend at the top. Differences between experimental groups and uninfected mice were analyzed by a two-way ANOVA followed by Tukey's multiple comparison test. For all statistical analyses P < 0.0 5 was considered significant.

824 **Table 1.** Linear B-cell epitopes identified in the OmpT, Cah and Hes proteins

Protein	Epitope name	Epitope Mapping	*In silico* B-cell prediction tools			Reactivity to HUS sera by ELISA. No (%)		Reactivity to control sera by ELISA. No (%)	
			BepiPred 2.0	Kolaskar and Tongaonker	Ellipro	IgG	IgA	IgG	IgA
OmpT	OmpT_1	Yes	Yes	No	Yes	17/20 (85)	5/7 (71)	0/3 (0)	0/3 (0)
	OmpT_2	Yes	Yes	No	Yes	18/20 (90)	5/7 (71)	0/3 (0)	0/3 (0)
	OmpT_3	Yes	Yes	Yes	Yes	16/20 (80)	6/7 (86)	0/3 (0)	0/3 (0)
	OmpT_4	Yes	Yes	Yes	Yes	18/20 (90)	3/7 (43)	0/3 (0)	0/3 (0)
	OmpT_5	Yes	Yes	No	Yes	16/20 (80)	4/7 (57)	0/3 (0)	0/3 (0)
	OmpT_6	Yes	Yes	No	Yes	18/20 (90)	5/7 (71)	0/3 (0)	0/3 (0)
Cah	Cah_1	Yes	Yes	Yes	Yes	18/20 (90)	3/7 (43)	0/3 (0)	0/3 (0)
	Cah_2	Yes	No	No	No	16/20 (80)	2/7 (29)	0/3 (0)	0/3 (0)
	Cah_3	Yes	Yes	No	Yes	19/20 (95)	5/7 (71)	0/3 (0)	0/3 (0)
	Cah_4	Yes	No	No	No	16/20 (80)	5/7 (71)	0/3 (0)	0/3 (0)
	Cah_5	Yes	No	No	No	20/20 (100)	4/7 (57)	0/3 (0)	0/3 (0)
	Cah_6	Yes	No	No	No	20/20 (100)	6/7 (86)	0/3 (0)	0/3 (0)
Hes	Hes_1	Yes	Yes	No	Yes	14/20 (70)	5/7 (71)	0/3 (0)	0/3 (0)
	Hes_2	Yes	Yes	Yes	Yes	17/20 (85)	5/7 (71)	0/3 (0)	0/3 (0)
	Hes_3	Yes	Yes	No	Yes	14/20 (70)	N.E.	0/3 (0)	N.E.
	Hes_4	Yes	No	No	Yes	12/20 (60)	N.E.	0/3 (0)	N.E.
	Hes_5	Yes	Yes	No	Yes	20/20 (100)	7/7 (100)	0/3 (0)	0/3 (0)

825 N.E. Not evaluated

826

827 **Table 2.** Epitopes and chemical and physical properties of the chimeric proteins

Protein	B-cell epitopes	Predicted T-cell epitopes	MW (kDa)	Theoretical pI	Solubility [1]	Estimated half-life [2]	Instability index [3]
Chimera 1	OmpT_1, OmpT_2, OmpT_3, OmpT_4, Hes_1, Hes_2, Hes_3 and Hes_5	Two of OmpT	29.6	4.51	0.693	>10 hours	21.30
Chimera 2	OmpT_1, OmpT_6, Cah_1, Cah_2, Cah_3, Cah_4, Cah_5, Cah_6, Hes_1, Hes_2 and Hes_5	Two of Cah	56.7	4.52	0.666	>10 hours	8.02

828

829 [1] Predicted by Protein-Sol tool [69]. Scaled solubility value (0-1). A value greater than 0.45 predicts that the protein is soluble.
830 [2] Prediction of the time it takes for half of the amount of protein in *E. coli* to disappear after its synthesis. [3] The instability
831 index provides an estimate of the stability of a protein in a test tube. A protein whose instability index is smaller than 40 is
832 predicted as stable [77].

833

834 **Table 3.** Intestinal colonization of STEC O157:H7 and protection conferred by
835 immunization with chimeric proteins

Chimeric protein + Adjuvant	Log10 CFU of STEC O157:H7 in Cecum (mean ± SD)	Log10 units of protection
Chi1 + Imject Alum	5.45 ± 0.24	0
Chi1 + Sigma Adjuvant	4.70 ± 0.56	0.68
Chi2 + Imject Alum	5.08 ± 0.54	0.30
Chi2 + Sigma Adjuvant	4.70 ± 0.86	0.68
Chi1 + Chi2 + Imject Alum	3.28 ± 0.10	2.10 *
Chi1 + Chi2 + Imject Alum	4.94 ± 0.81	0.44
PBS + Imject Alum + Sigma Adjuvant	5.38 ± 0.24	0

836 * $P < 0.001$ as compared to the control PBS group.

837

838

839 **Table 4.** Urinalysis clinical markers assessed at day 12 post-infection

Urinary marker	Chimeric protein + Adjuvant							Not challenged
	Chi1 + IA	Chi1 +SA	Chi2 + IA	Chi2 +SA	Chi1 + Chi2 + IA	Chi1 + Chi2 + SA	PBS + IA + SA	
Specific gravity	1,025	1,025	1,025	1,025	1,025	1,025	1,025	1,025
pH	6	6	6	6	6	6	6	6
Leukocytes (cells/µl)	75	25	75	25	75	25	500	25
Nitrite	Positive	Positive	Positive	Positive	Positive	Positive	Positive	Positive
Protein	Negative	Negative	Negative	Negative	Negative	Negative	Negative	Negative
Glucose (mmol/l)	2.8	2.8	2.8	2.8	2.8	2.8	2.8	2.8
Ketones	Negative	Negative	Negative	Negative	Negative	Negative	Negative	Negative
Urobilinogen (µmol/l)	Normal	Normal	17	Normal	17	Normal	70	Normal
Bilirubin	3+	3+	3+	3+	3+	3+	3+	3+
Blood	Negative	Negative	Negative	Negative	Negative	Negative	Negative	Negative

840

841

842

843

844

845

846

847

848

849

850

851

852

853

854

855

856

857

858

859

Funding and acknowledgments

This study was supported by FONDEF ID16I10140 and FONDECYT 1161161 grants. We thank Dr. Helen Lowry for the careful revision and edition of the manuscript. We thank Dr. Mauricio Farfan for sharing the STEC O157:H7 str. 86-24.

Conflict of interest

Currently, an application for an international patent had been presented for the chimeric antigens developed and uses thereof.

Author contributions

Conceptualization and experimental design: Roberto Vidal, David A. Montero, Felipe Del Canto, Juan C. Salazar and Angel Oñate. Data acquisition: Sandra Céspedes, Leandro Cádiz, José Reyes, Mauricio Arenas and David A. Montero. Data analysis and interpretation: Roberto Vidal, David A. Montero, Felipe Del Canto, Juan C. Salazar and Angel Oñate. Writing – original draft: David A. Montero; Review and edition: Roberto Vidal, Felipe Del Canto, Juan C. Salazar, Mauricio Arenas and Angel Oñate.

895 **References**

896 1 Nataro JP, Kaper JB. Diarrheagenic Escherichia coli. *Clin Microbiol Rev* 1998;
897 **11**: 142–201.

898 2 Freedman SB, Xie J, Neufeld MS, Hamilton WL, Hartling L, Tarr PI. Shiga
899 Toxin–Producing Escherichia coli Infection, Antibiotics, and Risk of Developing
900 Hemolytic Uremic Syndrome: A Meta-analysis. *Clin Infect Dis* 2016; **62**: 1251–
901 1258.

902 3 Majowicz SE, Scallan E, Jones-Bitton A, Sargeant JM, Stapleton J, Angulo FJ *et*
903 *al.* Global incidence of human Shiga toxin–producing Escherichia coli infections
904 and deaths: A systematic review and knowledge synthesis. *Foodborne Pathog*
905 *Dis* 2014; **11**: 447–455.

906 4 Hazard Identification and Characterization: Criteria for Categorizing Shiga
907 Toxin–Producing Escherichia coli on a Risk Basis †. *J Food Prot* 2019; **82**: 7–21.

908 5 Lee MS, Tesh VL. Roles of shiga toxins in immunopathology. *Toxins (Basel)*
909 2019; **11**: 1–26.

910 6 Farfan MJ, Torres AG. Molecular mechanisms that mediate colonization of Shiga
911 toxin-producing Escherichia coli strains. *Infect Immun* 2012; **80**: 903–913.

912 7 Montero DA, Velasco J, Del Canto F, Puente JL, Padola NL, Rasko DA *et al.*
913 Locus of Adhesion and Autoaggregation (LAA), a pathogenicity island present in
914 emerging Shiga Toxin-producing Escherichia coli strains. *Sci Rep* 2017; **7**: 7011.

915 8 Montero DA, Canto F Del, Velasco J, Colello R, Padola NL, Salazar JC *et al.*
916 Cumulative acquisition of pathogenicity islands has shaped virulence potential
917 and contributed to the emergence of LEE-negative Shiga toxin-producing
918 Escherichia coli strains. *Emerg Microbes Infect* 2019; **8**: 486–502.

919 9 Coombes BK, Wickham ME, Mascarenhas M, Gruenheid S, Finlay BB, Karmali
920 M a. Molecular analysis as an aid to assess the public health risk of non-O157
921 shiga toxin-producing Escherichia coli strains. *Appl Environ Microbiol* 2008; **74**:
922 2153–2160.

923 10 O'Ryan M, Vidal R, del Canto F, Carlos Salazar J, Montero D. Vaccines for viral
924 and bacterial pathogens causing acute gastroenteritis: Part II: Vaccines for
925 Shigella , Salmonella, enterotoxigenic E. coli (ETEC) enterohemorragic E. coli
926 (EHEC) and Campylobacter jejuni. *Hum Vaccin Immunother* 2015; **11**: 601–619.

927 11 Montero D, Orellana P, Gutiérrez D, Araya D, Salazar JC, Prado V *et al.*
928 Immunoproteomic analysis to identify Shiga toxin-producing Escherichia coli
929 outer membrane proteins expressed during human infection. *Infect Immun* 2014;
930 **82**: 4767–77.

931 12 Garcia-Angulo V a, Kalita A, Torres AG. Advances in the development of
932 enterohemorrhagic Escherichia coli vaccines using murine models of infection.
933 *Vaccine* 2013; **31**: 3229–35.

934 13 Cai K, Gao X, Li T, Wang Q, Hou X, Tu W *et al.* Enhanced immunogenicity of a
935 novel Stx2Am-Stx1B fusion protein in a mice model of enterohemorrhagic
936 Escherichia coli O157:H7 infection. *Vaccine* 2011; **29**: 946–952.

937 14 Mejias MP, Ghersi G, Craig PO, Panek CA, Bentancor L V, Baschkier A *et al.*
938 Immunization with a chimera consisting of the B subunit of Shiga toxin type 2
939 and brucella lumazine synthase confers total protection against Shiga toxins in
940 mice. *J Immunol* 2013; **191**: 2403–2411.

941 15 Martorelli L, Garimano N, Fiorentino GA, Vilte DA, Garbaccio SG, Barth SA *et al.*
942 Efficacy of a recombinant Intimin, EspB and Shiga toxin 2B vaccine in calves
943 experimentally challenged with Escherichia coli O157:H7. *Vaccine* 2018; **36**:
944 3949–3959.

945 16 Gu J, Liu Y, Yu S, Wang H, Wang Q, Yi Y *et al.* Enterohemorrhagic Escherichia
946 coli trivalent recombinant vaccine containing EspA, intimin and Stx2 induces
947 strong humoral immune response and confers protection in mice. *Microbes*
948 *Infect* 2009; **11**: 835–841.

949 17 Cheng Y, Feng Y, Luo P, Gu J, Yu S, Zhang W *et al.* Fusion expression and
950 immunogenicity of EHEC EspA-Stx2AI protein: implications for the vaccine
951 development. *J Microbiol* 2009; **47**: 498–505.

952 18 Gao X, Cai K, Li T, Wang Q, Hou X, Tian R *et al.* Novel fusion protein protects
953 against adherence and toxicity of enterohemorrhagic Escherichia coli O157:H7
954 in mice. *Vaccine* 2011; **29**: 6656–63.

955 19 Wan C, Zhou Y, Yu Y, Peng LJ, Zhao W, Zheng X. B-cell epitope KT-12 of
956 enterohemorrhagic Escherichia coli O157:H7: a novel peptide vaccine
957 candidate. *Microbiol Immunol* 2011; **55**: 247–53.

958 20 Liu J, Sun Y, Feng S, Zhu L, Guo X, Qi C. Towards an attenuated
959 enterohemorrhagic Escherichia coli O157:H7 vaccine characterized by a deleted

960 ler gene and containing apathogenic Shiga toxins. *Vaccine* 2009; **27**: 5929–
961 5935.

962 21 Cai K, Tu W, Liu Y, Li T, Wang H. Novel fusion antigen displayed-bacterial
963 ghosts vaccine candidate against infection of Escherichia coli O157:H7. *Sci Rep*
964 2015; **5**: 17479.

965 22 García-Angulo VA, Kalita A, Kalita M, Lozano L, Torres AG. Comparative
966 genomics and immunoinformatics approach for the identification of vaccine
967 candidates for enterohemorrhagic Escherichia coli O157:H7. *Infect Immun* 2014;
968 **82**: 2016–2026.

969 23 Riquelme-Neira R, Rivera A, Sáez D, Fernández P, Osorio G, del Canto F *et al.*
970 Vaccination with DNA Encoding Truncated Enterohemorrhagic Escherichia coli
971 (EHEC) Factor for Adherence-1 Gene (efa-1′) Confers Protective Immunity to
972 Mice Infected with E. coli O157:H7. *Front Cell Infect Microbiol* 2016; **5**: 1–9.

973 24 Escherichia E. Development of a Gold Nanoparticle Vaccine against. 2019; **10**:
974 1–16.

975 25 John M, Kudva IT, Griffin RW, Dodson AW, McManus B, Krastins B *et al.* Use of
976 in vivo-induced antigen technology for identification of Escherichia coli O157:H7
977 proteins expressed during human infection. *Infect Immun* 2005; **73**: 2665–79.

978 26 Colello R, Vélez MV, González J, Montero DA, Bustamante A V, Canto F Del *et*
979 *al.* First report of the distribution of Locus of Adhesion and Autoaggregation
980 (LAA) pathogenicity island in LEE-negative Shiga toxin-producing Escherichia
981 coli isolates from Argentina. *Microb Pathog* 2018; **123**: 259–263.

982 27 Carpenter EP, Beis K, Cameron AD, Iwata S. Overcoming the challenges of
983 membrane protein crystallography. *Curr Opin Struct Biol* 2008; **18**: 581–586.

984 28 Kaumaya PTP, Kobs-Conrad S, Seo YH, Lee H, Vanbuskirk AM, Feng N *et al.*
985 Peptide vaccines incorporating a ‘promiscuous’ T-cell epitope bypass certain
986 haplotype restricted immune responses and provide broad spectrum
987 immunogenicity. *J Mol Recognit* 1993; **6**: 81–94.

988 29 Reed SG, Orr MT, Fox CB. Key roles of adjuvants in modern vaccines. *Nat Med*
989 2013; **19**: 1597–1608.

990 30 Mohanan D, Slütter B, Henriksen-Lacey M, Jiskoot W, Bouwstra JA, Perrie Y *et*
991 *al.* Administration routes affect the quality of immune responses: A cross-

992 sectional evaluation of particulate antigen-delivery systems. *J Control Release*
993 2010; **147**: 342–349.

994 31 Belyakov IM, Ahlers JD. What Role Does the Route of Immunization Play in the
995 Generation of Protective Immunity against Mucosal Pathogens? *J Immunol*
996 2009; **183**: 6883–6892.

997 32 Melton-Celsa AR, O'Brien AD, Feng PCH. Virulence Potential of Activatable
998 Shiga Toxin 2d-Producing Escherichia coli Isolates from Fresh Produce. *J Food*
999 *Prot* 2015; **78**: 2085–2088.

1000 33 Melton-Celsa AR, Darnell SC, O'Brien AD. Activation of Shiga-like toxins by
1001 mouse and human intestinal mucus correlates with virulence of
1002 enterohemorrhagic Escherichia coli O91:H21 isolates in orally infected,
1003 streptomycin-treated mice. *Infect Immun* 1996; **64**: 1569–76.

1004 34 Cox MMJ. Recombinant protein vaccines produced in insect cells. *Vaccine* 2012;
1005 **30**: 1759–1766.

1006 35 Hollingshead S, Jongerius I, Exley RM, Johnson S, Lea SM, Tang CM.
1007 Structure-based design of chimeric antigens for multivalent protein vaccines. *Nat*
1008 *Commun* 2018; **9**: 1–10.

1009 36 Li W, Joshi M, Singhania S, Ramsey K, Murthy A. Peptide Vaccine: Progress
1010 and Challenges. *Vaccines* 2014; **2**: 515–536.

1011 37 Chang YF, Chen CS, Palaniappan RUM, He H, McDonough SP, Barr SC *et al.*
1012 Immunogenicity of the recombinant leptospiral putative outer membrane proteins
1013 as vaccine candidates. *Vaccine* 2007; **25**: 8190–8197.

1014 38 Tapia D, Ross BN, Kalita A, Kalita M, Hatcher CL, Muruato LA *et al.* From In
1015 silico Protein Epitope Density Prediction to Testing Escherichia coli O157:H7
1016 Vaccine Candidates in a Murine Model of Colonization. *Front Cell Infect*
1017 *Microbiol* 2016; **6**: 1–8.

1018 39 Wells TJ, Tree JJ, Ulett GC, Schembri M a. Autotransporter proteins: novel
1019 targets at the bacterial cell surface. *FEMS Microbiol Lett* 2007; **274**: 163–72.

1020 40 Harris J a., Roy K, Woo-Rasberry V, Hamilton DJ, Kansal R, Qadri F *et al.*
1021 Directed Evaluation of Enterotoxigenic Escherichia coli Autotransporter Proteins
1022 as Putative Vaccine Candidates. *PLoS Negl Trop Dis* 2011; **5**: e1428.

1023 41 Klein NP. Licensed pertussis vaccines in the United States. *Hum Vaccin*

1024 *Immunother* 2014; **10**: 2684–2690.

1025 42 Brandtzaeg P. Mucosal immunity: Induction, dissemination, and effector
1026 functions. *Scand J Immunol* 2009; **70**: 505–515.

1027 43 Eckmann L, Stappenbeck TS. IgG 'detoxes' the intestinal mucosa. *Cell Host*
1028 *Microbe* 2015; **17**: 538–9.

1029 44 Horton RE, Vidarsson G. Antibodies and Their Receptors: Different Potential
1030 Roles in Mucosal Defense. *Front Immunol* 2013; **4**.
1031 doi:10.3389/fimmu.2013.00200.

1032 45 Kamada N, Sakamoto K, Seo S-U, Zeng MY, Kim Y-G, Cascalho M *et al.*
1033 Humoral Immunity in the Gut Selectively Targets Phenotypically Virulent
1034 Attaching-and-Effacing Bacteria for Intraluminal Elimination. *Cell Host Microbe*
1035 2015; **17**: 617–27.

1036 46 Westerman LE, McClure HM, Jiang B, Almond JW, Glass RI. Serum IgG
1037 mediates mucosal immunity against rotavirus infection. *Proc Natl Acad Sci* 2005;
1038 **102**: 7268–7273.

1039 47 Amani J, Salmanian AH, Rafati S, Mousavi SL. Immunogenic properties of
1040 chimeric protein from espA, eae and tir genes of Escherichia coli O157:H7.
1041 *Vaccine* 2010; **28**: 6923–6929.

1042 48 Kolling GL, Matthews KR. Export of virulence genes and Shiga toxin by
1043 membrane vesicles of Escherichia coli O157:H7. *Appl Environ Microbiol* 1999;
1044 **65**: 1843–1848.

1045 49 Kim SH, Lee SR, Kim KS, Ko A, Kim E, Kim YH *et al.* Shiga toxin A subunit
1046 mutant of Escherichia coli O157:H7 releases outer membrane vesicles
1047 containing the B-pentameric complex. *FEMS Immunol Med Microbiol* 2010; **58**:
1048 412–420.

1049 50 Kunsmann L, Rüter C, Bauwens A, Greune L, Glüder M, Kemper B *et al.*
1050 Virulence from vesicles: Novel mechanisms of host cell injury by Escherichia coli
1051 O104:H4 outbreak strain. 2015. doi:10.1038/srep13252.

1052 51 Bielaszewska M, Rü Ter 2 C, Bauwens A, Greune L, Jarosch K-A, Steil D *et al.*
1053 Host cell interactions of outer membrane vesicle-associated virulence factors of
1054 enterohemorrhagic Escherichia coli O157: Intracellular delivery, trafficking and
1055 mechanisms of cell injury. 2017. doi:10.1371/journal.ppat.1006159.

1056 52 Watanabe-Takahashi M, Yamasaki S, Murata M, Kano F, Motoyama J, Yamate
1057 J *et al.* Exosome-associated Shiga toxin 2 is released from cells and causes
1058 severe toxicity in mice. *Sci Rep* 2018; **8**: 10776.

1059 53 Boysen A, Borch J, Krogh J, Hjernø K, Møller-Jensen J. SILAC-based
1060 comparative analysis of pathogenic Escherichia coli secretomes. *J Microbiol*
1061 *Methods* 2015; **116**: 66–79.

1062 54 Premjani V, Tilley D, Gruenheid S, Le Moual H, Samis JA. Enterohemorrhagic
1063 Escherichia coli OmpT regulates outer membrane vesicle biogenesis. 2014.
1064 doi:10.1111/1574-6968.12463.

1065 55 Ralli-Jain P, Tifrea D, Cheng C, Pal S, de la Maza LM. Enhancement of the
1066 protective efficacy of a Chlamydia trachomatis recombinant vaccine by
1067 combining systemic and mucosal routes for immunization. *Vaccine* 2010; **28**:
1068 7659–7666.

1069 56 Vajdy M, Singh M, Ugozzoli M, Briones M, Soenawan E, Cuadra L *et al.*
1070 Enhanced mucosal and systemic immune responses to Helicobacter pylori
1071 antigens through mucosal priming followed by systemic boosting immunizations.
1072 *Immunology* 2003; **110**: 86–94.

1073 57 Kim Y, Ponomarenko J, Zhu Z, Tamang D, Wang P, Greenbaum J *et al.* Immune
1074 epitope database analysis resource. *Nucleic Acids Res* 2012; **40**: 525–530.

1075 58 Jespersen MC, Peters B, Nielsen M, Marcatili P. BepiPred-2.0: Improving
1076 sequence-based B-cell epitope prediction using conformational epitopes. *Nucleic*
1077 *Acids Res* 2017; **45**: W24–W29.

1078 59 Kolaskar a S, Tongaonkar PC. A semi-empirical method for prediction of
1079 antigenic determinants on protein antigens. *FEBS Lett* 1990; **276**: 172–4.

1080 60 Ponomarenko J, Bui H-H, Li W, Fusseder N, Bourne PE, Sette A *et al.* ElliPro: a
1081 new structure-based tool for the prediction of antibody epitopes. *BMC*
1082 *Bioinformatics* 2008; **9**: 514.

1083 61 Horst R, Stanczak P, Wüthrich K. NMR Polypeptide Backbone Conformation of
1084 the E. coli Outer Membrane Protein W. *Structure* 2014; **22**: 1204–1209.

1085 62 Vandeputte-Rutten L, Kramer RA, Kroon J, Dekker N, Egmond MR, Gros P.
1086 Crystal structure of the outer membrane protease Ompt from Escherichia coli
1087 suggests a novel catalytic site. *EMBO J* 2001; **20**: 5033–5039.

1088 63 Heras B, Totsika M, Peters KM, Paxman JJ, Gee CL, Jarrott RJ. The antigen 43
1089 structure reveals a molecular Velcro- like mechanism of autotransporter-
1090 mediated bacterial clumping. 2014; **111**: 457–462.

1091 64 Sánchez R, Šali A. Evaluation of comparative protein structure modeling by
1092 MODELLER-3. *Proteins Struct Funct Genet* 1997; **29**: 50–58.

1093 65 Ricker EW. Stoch and Recruitrnent. *J Fish Res Board Canada* 1954; **11**: 559–
1094 623.

1095 66 Biller JR, Elajaili H, Meyer V, Rosen GM, Eaton SS, Eaton GR. Electron spin–
1096 lattice relaxation mechanisms of rapidly-tumbling nitroxide radicals. *J Magn*
1097 *Reson* 2013; **236**: 47–56.

1098 67 Foloppe N, Mackerell AD. Acids : I . Parameter Optimization Based on Small
1099 Molecule and Condensed Phase Macromolecular Target Data. *J Comput Chem*
1100 2000; **21**: 86–104.

1101 68 Wiederstein M, Sippl MJ. ProSA-web: Interactive web service for the recognition
1102 of errors in three-dimensional structures of proteins. *Nucleic Acids Res* 2007; **35**:
1103 407–410.

1104 69 Hebditch M, Carballo-Amador MA, Charonis S, Curtis R, Warwicker J. Protein-
1105 Sol: A web tool for predicting protein solubility from sequence. *Bioinformatics*
1106 2017; **33**: 3098–3100.

1107 70 Wilkins MR, Gasteiger E, Bairoch A, Sanchez JC, Williams KL, Appel RD *et al.*
1108 Protein identification and analysis tools in the ExPASy server. *Methods Mol Biol*
1109 1999; **112**: 531–552.

1110 71 Pettersen EF, Goddard TD, Huang CC, Couch GS, Greenblatt DM, Meng EC *et*
1111 *al.* UCSF Chimera - A visualization system for exploratory research and
1112 analysis. *J Comput Chem* 2004; **25**: 1605–1612.

1113 72 Wadolkowski E a., Burris J a., O'Brien a. D. Mouse model for colonization and
1114 disease caused by enterohemorrhagic Escherichia coli O157:H7. *Infect Immun*
1115 1990; **58**: 2438–45.

1116 73 Lindgren SW, Melton AR, O'Brien AD. Virulence of enterohemorrhagic
1117 Escherichia coli O91:H21 clinical isolates in an orally infected mouse model.
1118 *Infect Immun* 1993; **61**: 3832–42.

1119 74 Kurien BT, Hal Scofield R. Mouse urine collection using clear plastic wrap. *Lab*

Anim 1999; **33**: 83–86.

75 Warnes GR, Bolker B, Bonebakker L, Gentleman R, Huber W, Lumley T *et al.* R Package ‘ gplots ’. 2016.https://cran.r-project.org/web/packages/gplots/gplots.pdf.

76 R Core Team. *R: A Language and Environment for Statistical Computing*. R Foundation for Statistical Computing. Vienna, Austria., 2014http://www.r-project.org.

77 Guruprasad K, Reddy BVB, Pandit MW. Correlation between stability of a protein and its dipeptide composition: A novel approach for predicting in vivo stability of a protein from its primary sequence. *Protein Eng Des Sel* 1990; **4**: 155–161.

(a) Antigens

OmpT Cah Hes

- Reactive to IgG and IgA from HUS sera
- Expressed during human infection
- Widespread among clinical STEC strains
- Mainly absent in commensal *E. coli* strains

(b) Identification and validation of epitopes

- Epitope mapping

overlapping peptides

- *In silico* prediction of B and T cell epitopes

Sera from patients

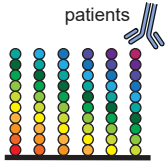

Peptide microarray

- Validation of B-cell epitopes by ELISA

(c) Design and purification of chimeric proteins

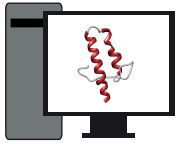

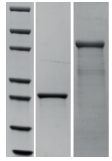

Chimera 1 (Chi1):
8 B-cell epitopes
2 MCH-II epitopes

Chimera 2 (Chi2):
11 B-cell epitopes
2 MHC-II epitopes

- Confirmation of seroreactivity of chimeras by ELISA

(d) Immunization, determination of immune responses and challenge experiments

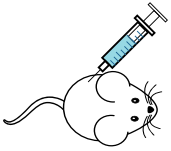

Intramuscular immunization

vs.

BALB/c

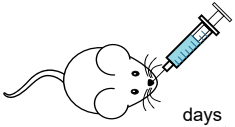

Intrasal immunization

Group 1: Chi1 + IA
Group 3: Chi2 + IA
Group 5: Chi1 + Chi2 + IA
Group 7: PBS + IA + SA

Group 2: Chi1 + SA
Group 4: Chi2 + SA
Group 6: Chi1 + Chi2 + SA

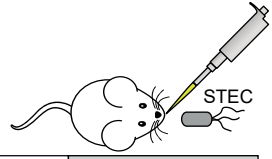

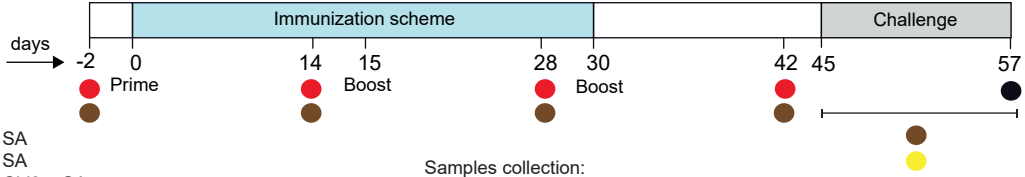

Samples collection:

- Blood
- Feces
- Urine
- Organs

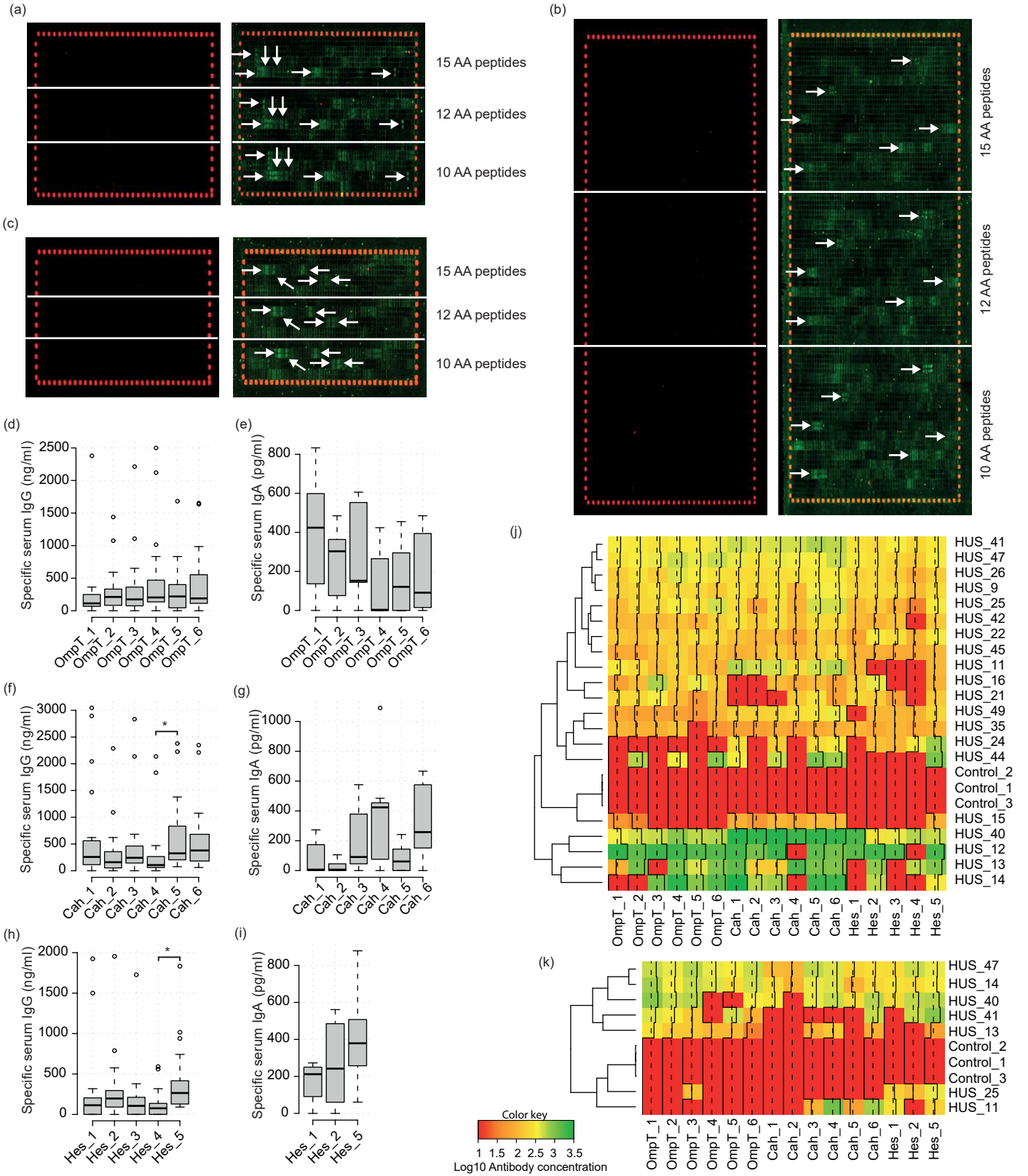
(a)
15 AA peptides
12 AA peptides
10 AA peptides
(b)
15 AA peptides
12 AA peptides
10 AA peptides
(c)
15 AA peptides
12 AA peptides
10 AA peptides
(d)
Specific serum IgG (ng/ml)
OmpT_1
OmpT_2
OmpT_3
OmpT_4
OmpT_5
OmpT_6
(e)
Specific serum IgA (pg/ml)
(f)
Specific serum IgG (ng/ml)
Cah_1
Cah_2
Cah_3
Cah_4
Cah_5
Cah_6
(g)
Specific serum IgA (pg/ml)
(h)
Specific serum IgG (ng/ml)
Hes_1
Hes_2
Hes_3
Hes_4
Hes_5
(i)
Specific serum IgA (pg/ml)
(j)
HUS_41
HUS_47
HUS_26
HUS_9
HUS_25
HUS_42
HUS_22
HUS_45
HUS_11
HUS_16
HUS_21
HUS_49
HUS_35
HUS_24
HUS_44
Control_2
Control_1
Control_3
HUS_15
HUS_40
HUS_12
HUS_13
HUS_14
(k)
HUS_47
HUS_14
HUS_40
HUS_41
HUS_13
Control_2
Control_1
Control_3
HUS_25
HUS_11
Color key
1 1.5 2 2.5 3 3.5
Log10 Antibody concentration

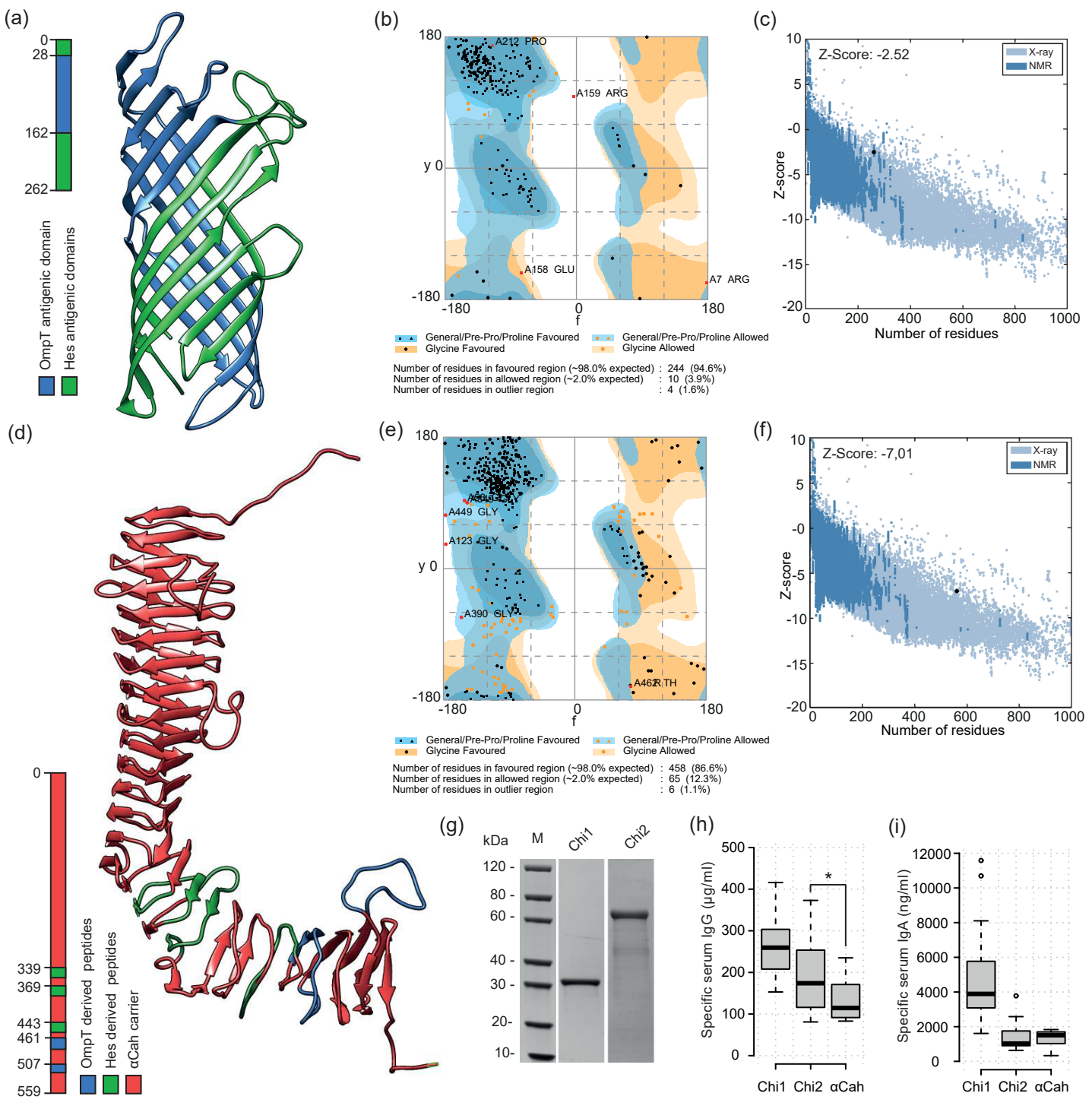
(a)
0
28
162
262
OmpT antigenic domain
Hes antigenic domains
(b)
180
A212 PRO
A159 ARG
y 0
A158 GLU
A7 ARG
-180
-180
0
180
f
General/Pre-Pro/Proline Favoured
General/Pre-Pro/Proline Allowed
Glycine Favoured
Glycine Allowed
Number of residues in favoured region (~98.0% expected) : 244 (94.6%)
Number of residues in allowed region (~2.0% expected) : 10 (3.9%)
Number of residues in outlier region : 4 (1.6%)
(c)
Z-Score: -2.52
X-ray
NMR
Z-score
Number of residues
(d)
0
339
369
443
461
507
559
OmpT derived peptides
Hes derived peptides
αCah carrier
(e)
180
A449 GLY
A123 GLY
y 0
A390 GLY
A462 THR
-180
-180
0
180
f
General/Pre-Pro/Proline Favoured
General/Pre-Pro/Proline Allowed
Glycine Favoured
Glycine Allowed
Number of residues in favoured region (~98.0% expected) : 458 (86.6%)
Number of residues in allowed region (~2.0% expected) : 65 (12.3%)
Number of residues in outlier region : 6 (1.1%)
(f)
Z-Score: -7,01
X-ray
NMR
Z-score
Number of residues
(g)
kDa
M
Chi1
Chi2
120 -
80 -
60 -
40 -
30 -
20-
10-
(h)
Specific serum IgG (µg/ml)
*
Chi1
Chi2
αCah
(i)
Specific serum IgA (ng/ml)
Chi1
Chi2
αCah

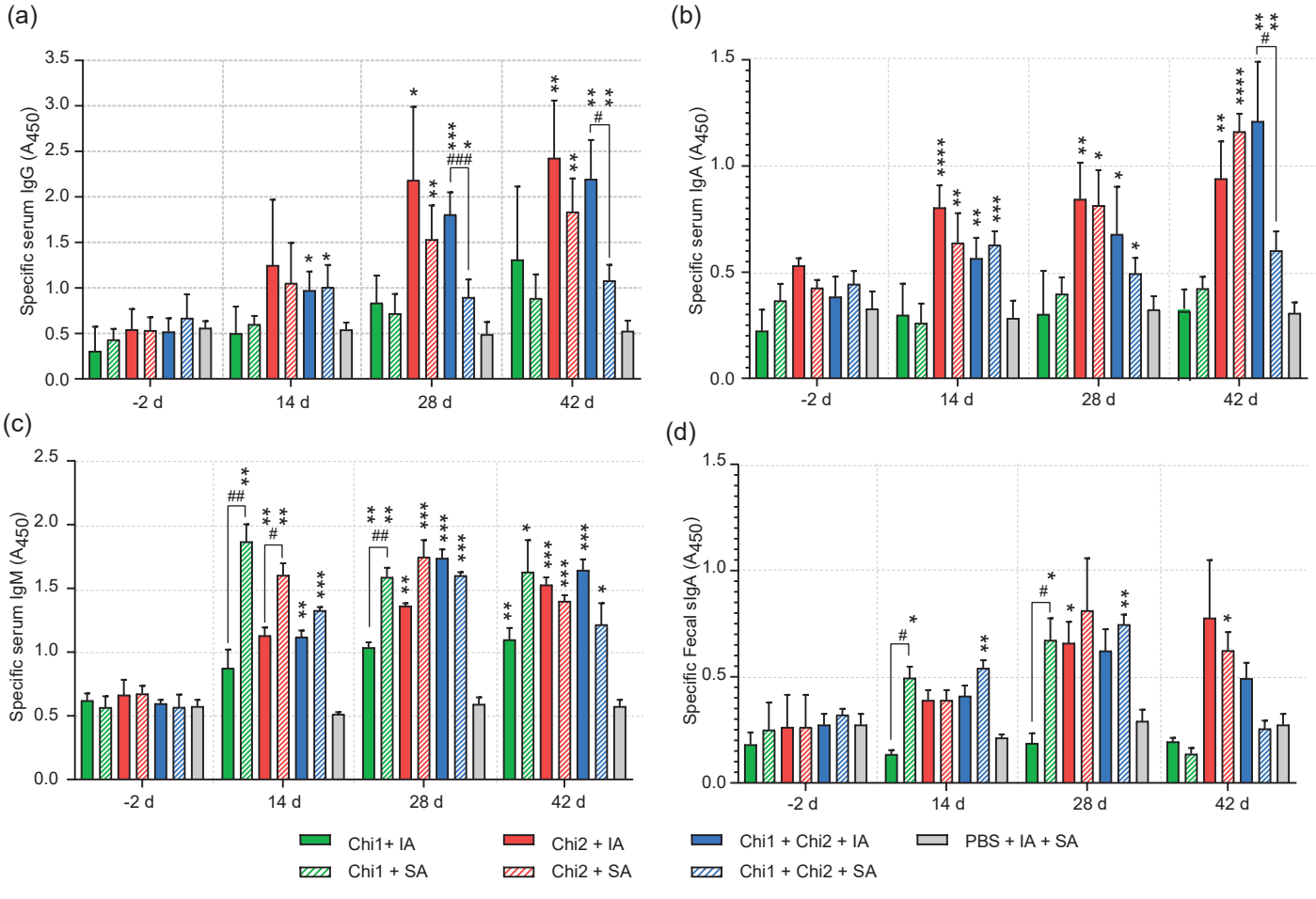
(a)
Specific serum IgG (A_{450})
3.5
3.0
2.5
2.0
1.5
1.0
0.5
0.0
-2 d
14 d
28 d
42 d
(b)
Specific serum IgA (A_{450})
1.5
1.0
0.5
0.0
-2 d
14 d
28 d
42 d
(c)
Specific serum IgM (A_{450})
2.5
2.0
1.5
1.0
0.5
0.0
-2 d
14 d
28 d
42 d
(d)
Specific Fecal sIgA (A_{450})
1.5
1.0
0.5
0.0
-2 d
14 d
28 d
42 d
Chi1+ IA
Chi1 + SA
Chi2 + IA
Chi2 + SA
Chi1 + Chi2 + IA
Chi1 + Chi2 + SA
PBS + IA + SA

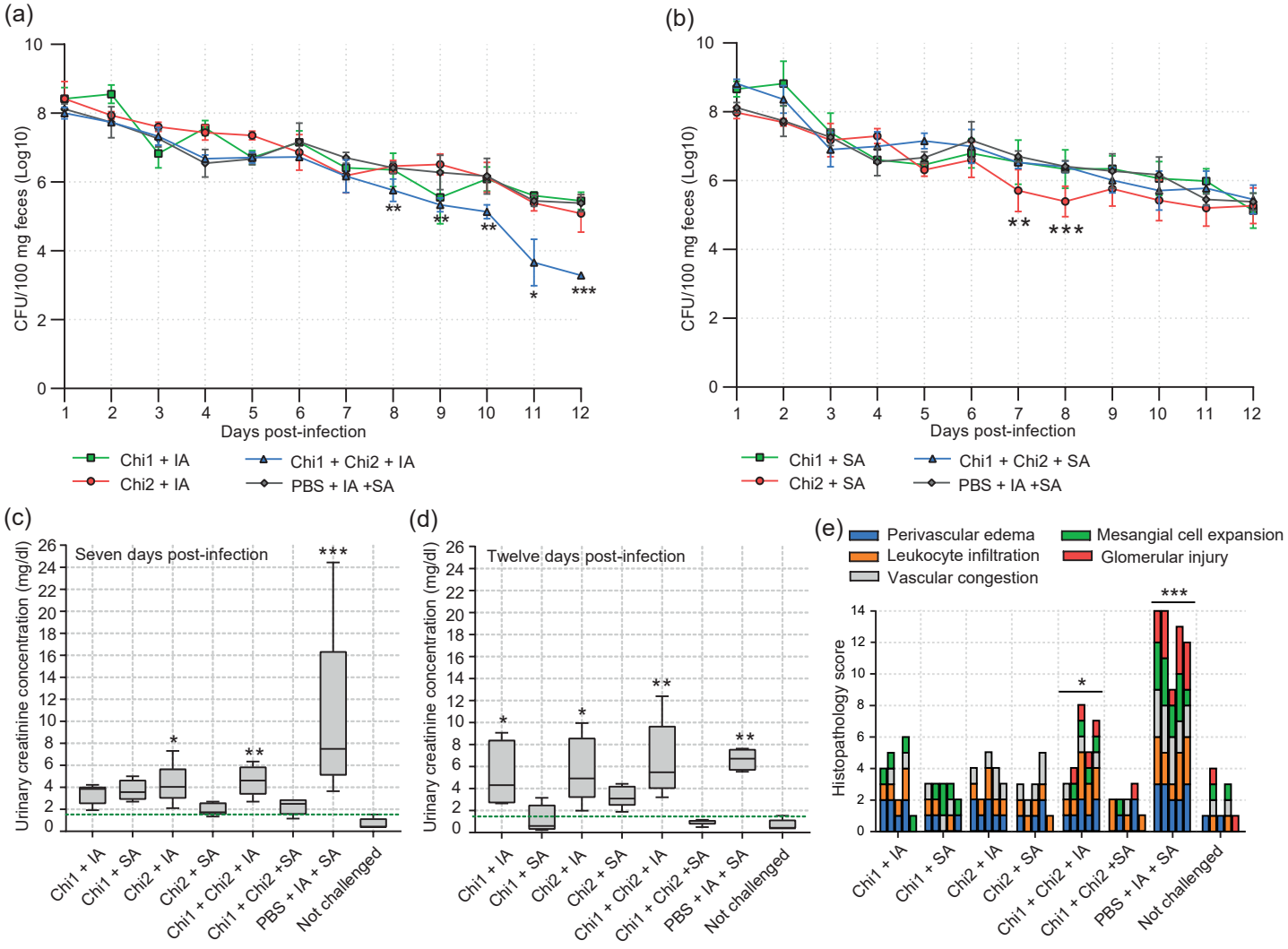
(a)
CFU/100 mg feces (Log10)
Days post-infection
Chi1 + IA
Chi2 + IA
Chi1 + Chi2 + IA
PBS + IA +SA
(b)
CFU/100 mg feces (Log10)
Days post-infection
Chi1 + SA
Chi2 + SA
Chi1 + Chi2 + SA
PBS + IA +SA
(c)
Seven days post-infection
Urinary creatinine concentration (mg/dl)
Chi1 + IA
Chi1 + SA
Chi2 + IA
Chi2 + SA
Chi1 + Chi2 + IA
Chi1 + Chi2 +SA
PBS + IA + SA
Not challenged
(d)
Twelve days post-infection
Urinary creatinine concentration (mg/dl)
(e)
Perivascular edema
Leukocyte infiltration
Vascular congestion
Mesangial cell expansion
Glomerular injury
Histopathology score